General Disclaimer

One or more of the Following Statements may affect this Document

- This document has been reproduced from the best copy furnished by the organizational source. It is being released in the interest of making available as much information as possible.

- This document may contain data, which exceeds the sheet parameters. It was furnished in this condition by the organizational source and is the best copy available.

- This document may contain tone-on-tone or color graphs, charts and/or pictures, which have been reproduced in black and white.

- This document is paginated as submitted by the original source.

- Portions of this document are not fully legible due to the historical nature of some of the material. However, it is the best reproduction available from the original submission.

Produced by the NASA Center for Aerospace Information (CASI)

NASA

Technical Memorandum **79722**

A Geophysical Atlas for Interpretation of Satellite - Derived Data

Paul D. Lowman Jr. and Herbert V. Frey

(NASA-TM-79722) A GEOPHYSICAL ATLAS FOR INTERPRETATION OF SATELLITE-DERIVED DATA (NASA) 60 p HC A04/MF A01 CSCL 08G

N79-20557

Unclas
G3/46 19635

FEBRUARY 1979

National Aeronautics and Space Administration

Goddard Space Flight Center
Greenbelt, Maryland 20771



A GEOPHYSICAL ATLAS
FOR INTERPRETATION OF SATELLITE-DERIVED DATA*

Edited By:

Paul D. Lowman, Jr.
Herbert V. Frey

Geophysics Branch
Goddard Space Flight Center
Greenbelt, Maryland 20771

Contributing Authors:

Albany Global Tectonics Group, W. M. Davis, H. V. Frey, A. P. Greenberg,
M. K. Hutchinson, R. A. Langel, P. D. Lowman, Jr., B. E. Lowrey,
J. G. Marsh, G. D. Mead, J. A. O'Keefe, and A. P. Trombka

February 1979

*Preliminary Version (see Editor's Note inside)

GODDARD SPACE FLIGHT CENTER
Greenbelt, Maryland 20771

Editorial Note

This publication is a preliminary version of the Atlas, published in reduced size. A larger version in folio size will be published shortly; when available, it can be obtained from the Geophysics Branch, Code 922, Goddard Space Flight Center, Greenbelt, Maryland 20771.

ORIGINAL PAGE IS
OF POOR QUALITY

TABLE OF CONTENTS

	Page
INTRODUCTION	1
P. D. Lowman, Jr., and H. V. Frey	
Plate 1: The Physical World	3
SECTION 1: BASE MAPS AND PROJECTIONS	5
J. A. O'Keefe, A. P. Greenberg, and G. D. Mead	
Plate 2: Van der Grinten Grid	8
SECTION 2: SATELLITE-DERIVED GRAVITY MAPS	9
J. G. Marsh	
Plate 3: Gravity Field Anomalies: Full Field	11
Plate 4: Free-Air Gravity Anomalies: Degree, Order 0 - 13	12
Plate 5: Free-Air Gravity Anomalies: Degree, Order 13 - 22	13
Plate 6: Gravimetric Geoid	14
SECTION 3: SATELLITE-DERIVED MAGNETIC ANOMALY MAPS	15
H. V. Frey, R. A. Langel, and W. M. Davis	
Plate 7: Scalar Magnetic Anomalies: Smoothed Version, Contoured	17
Plate 8: Scalar Magnetic Anomalies: Smoothed Version, Patterned	18
Plate 9: Scalar Magnetic Anomalies: Filtered Version, Patterned	19
SECTION 4: GLOBAL SEISMICITY MAPS	21
M. K. Hutchinson and P. D. Lowman, Jr.	
Plate 10: Seismic Epicenters: Without Continental Outlines	23
Plate 11: Seismic Epicenters: With Continental Outlines	24
Plate 12: Arctic Seismicity	25
Plate 13: Antarctic Seismicity	26
SECTION 5: RECENT VOLCANIC ACTIVITY MAP	27
A. P. Trombka and P. D. Lowman, Jr.	
Plate 14: Recent Volcanic Activity	30
SECTION 6: TECTONIC BOUNDARIES: RIFT AND SUTURE MAPS	31
H. V. Frey	
Plate 15: Tectonic Boundaries: Rifts	33
Plate 16: Tectonic Boundaries: Sutures	34

Page

SECTION 7: GLOBAL TECTONIC AND VOLCANIC ACTIVITY MAPS 35

P. D. Lowman, Jr.

Plate 17: Global Tectonic and Volcanic Activity 40
Plate 18: Tectonic and Volcanic Activity of the Arctic Regions 41
Plate 19: Tectonic and Volcanic Activity of the Antarctic Regions 42

SECTION 8: SEISMIC VELOCITY ANOMALY MAPS 43

B. E. Lowrey

Plate 20: Seismic Velocity Anomalies: Case 1, 0 - 670 km Depth 45
Plate 21: Seismic Velocity Anomalies: Case 1, 670 - 1100 km Depth 46
Plate 22: Seismic Velocity Anomalies: Case 1, 1100 - 1500 km Depth 47
Plate 23: Seismic Velocity Anomalies: Case 1, 1500 - 2200 km Depth 48
Plate 24: Seismic Velocity Anomalies: Case 1, 2200 - 2886 km Depth 49
Plate 25: Seismic Velocity Anomalies: Case 2, 0 - 670 km Depth 50
Plate 26: Seismic Velocity Anomalies: Case 2, 670 - 1100 km Depth 51
Plate 27: Seismic Velocity Anomalies: Case 2, 1100 - 1500 km Depth 52
Plate 28: Seismic Velocity Anomalies: Case 2, 1500 - 2200 km Depth 53
Plate 29: Seismic Velocity Anomalies: Case 2, 2200 - 2886 km Depth 54

A GEOPHYSICAL ATLAS
FOR INTERPRETATION OF SATELLITE-DERIVED DATA

Paul D. Lowman, Jr.
Herbert V. Frey

INTRODUCTION

Our knowledge of the earth's structure has increased tremendously in the last two decades, much more so than would be expected in the normal course of scientific progress. There are several reasons for this increase, one of them being the achievement of space flight, and specifically the launching of earth-orbiting artificial satellites. These satellites, either directly or indirectly, have permitted investigations of the earth's gravity field, crustal magnetism, plate movements, and crustal structure. We present here the first unified compilation of satellite-derived and conventional geophysical data applicable to such investigations.

This Atlas consists of a series of maps intended for qualitative intercomparison. Several of these, such as the maps showing global seismicity, are ground-based data necessary for interpretation of the satellite data. The maps have been drawn on a common projection (Van der Grinten) and with a common scale, except for those showing the polar regions, which use an orthographic projection. Each map represents the result of many years' work by many people and immense compilations of data (much of it digital), which would be impractical to reference completely. However, the main publications used are listed in the bibliography. In addition, the reader may find useful the "Directory of U.S. Data Repositories Supporting the International Geodynamics Project" (Report SE-14, World Data Center A, National Oceanic and Atmospheric Administration, Boulder, CO 80803, 1978).

The Atlas is intended as a tool for scientists and educators rather than as a research publication in itself. For this reason, the authors have included only brief accompanying texts for the maps, designed to aid the reader in their use. A brief summary of the content and organization of the Atlas follows.

The first map (Plate 1), reproduced with the kind permission of the National Geographic Society, shows the world's physiography, both continental and oceanic. This map was chosen as a topographic base because of its detailed representation of physiographic features such as ridges, trenches, and transform faults, the fact that it does not split any large land masses, and its Van der Grinten projection. The Van der Grinten projection, discussed in detail in Section 1, though neither equal-area nor conformal, permits the inclusion of very high latitudes with moderate distortion compared to the commonly-used Mercator projection. A Van der Grinten outline map with latitude and longitude is also presented (Plate 2). The first geophysical maps show various aspects of the earth's gravity field, a subject of fundamental importance and, historically, the first branch of geophysics to benefit from satellite-derived data. Next follow maps of the earth's crustal magnetism as measured by the Polar Orbiting Geophysical Observatory satellites. These are followed by a series of seismic activity maps, which are of interest both by themselves and because they served as a major input to other maps in the Atlas. Volcanic activity of the past one million years is shown both on a specialized map and later on a combined map of tectonic and volcanic activity. We then present maps of the earth's rifts and sutures, representing in plate tectonic theory the beginning and end of ocean basin evolution. These are followed by three maps showing global tectonic and volcanic activity for the past one million years. Finally, a series of ten maps shows seismic wave velocity anomalies for a set of five depth regions, from the surface to the core-mantle boundary at 2900 km depth.

Since this is the first such compilation of satellite-derived and related conventional geophysical data, much improvement in content and format is doubtless possible; we stress that this is a preliminary version and that improved editions will follow. We believe, however, that even this first edition of the Atlas will be useful as a research tool, an educational resource, and as a demonstration of the great scientific value of artificial satellites.

ACKNOWLEDGEMENTS

This Atlas represents the efforts of many people besides the authors. We particularly wish to thank the following for contributing to and advising on its preparation:

Richard J. Allenby, Geophysics Branch, Goddard Space Flight Center

Walter Alvarez, University of California

Phyllis S. Chovitz, EG&G, Washington Analytical Services Center, Inc.

Barbara M. Christy, Library of Congress

Adam M. Dziewonski, Harvard University

Gary Fitzgerald, Library of Congress

F. T. Heuring, formerly with Phoenix Corporation

F. J. Lerch, Geodynamics Branch, Goddard Space Flight Center

Barbara C. Lueders, Geophysics Branch, Goddard Space Flight Center

Michael A. Mayhew, Business and Technical Services, Inc.

John J. McCarthy, EG&G, Washington Analytical Services Center, Inc.

Stephen P. Meszaros, Presentations Section, Goddard Space Flight Center

The National Geographic Society, Washington, D.C.

James Ni, Cornell University

William T. Peele, formerly Chief Cartographer, National Geographic Society

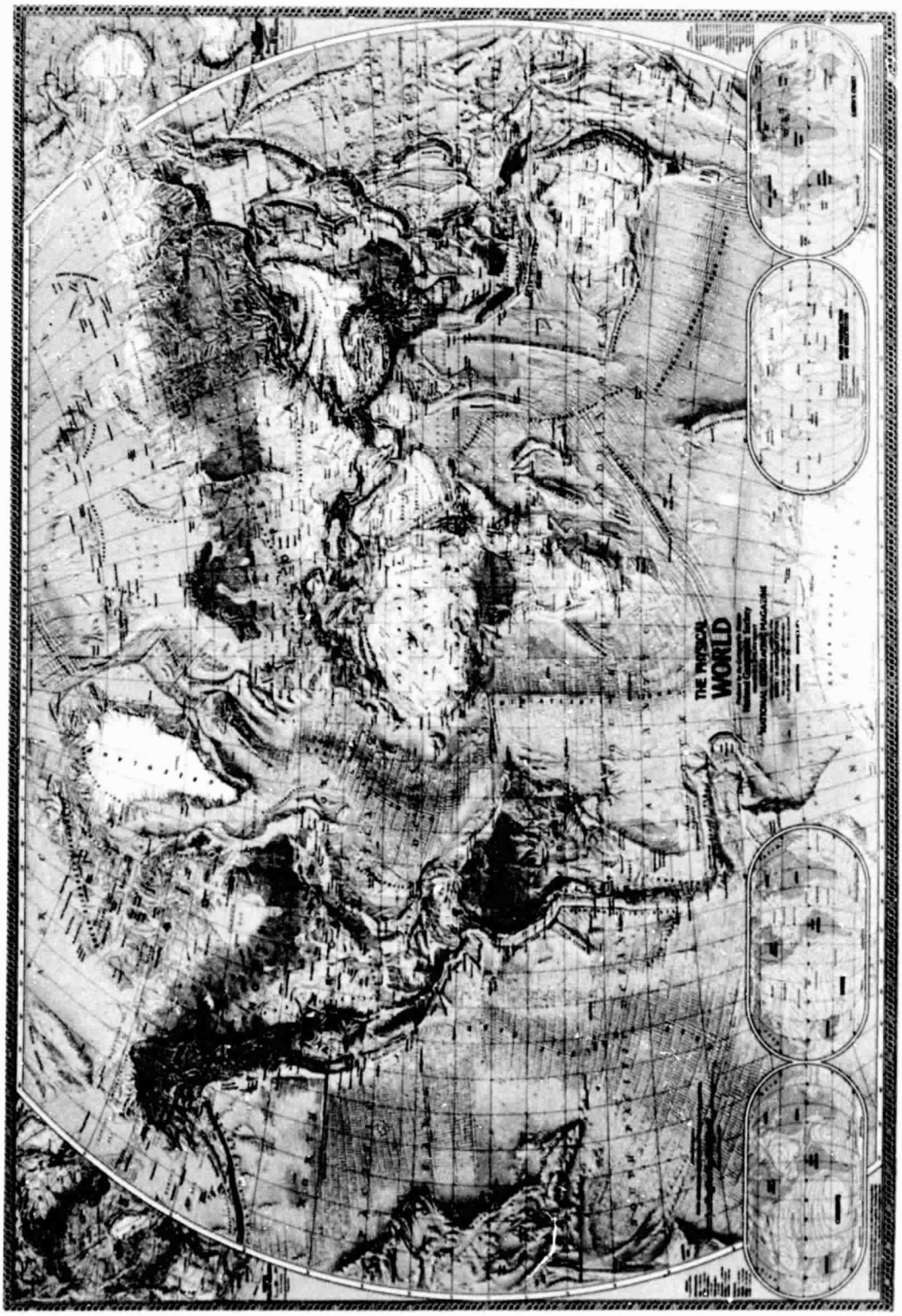
David P. Rubincam, Geodynamics Branch, Goddard Space Flight Center

David P. Smith, Geodynamics Branch, Goddard Space Flight Center

Patrick T. Taylor, Geophysics Branch, Goddard Space Flight Center

William J. Webster, Geophysics Branch, Goddard Space Flight Center

Louis S. Walter, Earth Survey Applications Division, Goddard Space Flight Center.



ORIGINAL PAGE IS
OF POOR QUALITY

SECTION 1: BASE MAPS AND PROJECTIONS

John O'Keefe, Allen Greenberg, and Gilbert Mead

Two projections have been used for all of the maps in this Atlas. For reasons given in the Introduction, most of the maps were plotted, all to the same scale, on the Van der Grinten projection (Van der Grinten, 1905). The remaining data were plotted using an orthographic polar projection. The mathematical characteristics of these two projections are given here for the benefit of those who may wish to plot additional data to the same scale and projection.

VAN DER GRINTEN PROJECTION

A latitude-longitude grid of the Van der Grinten projection is shown in Plate 2. This plate, as well as most of the plates in this Atlas using the Van der Grinten projection, extends only to latitude ±80°. The outline of the entire earth, including the poles, is a perfect circle. The projection has true scale along the equator. It is neither conformal nor equal-area. The characteristics of this projection were reviewed by O'Keefe and Greenberg (1977), who also derived analytic equations for the rectangular coordinates (x,y) of a point P whose longitude measured eastward is λ and whose latitude is ϕ. The final results are given here; for the specific derivation and the description of the projection as given initially by Van der Grinten, see O'Keefe and Greenberg (1977).

Suppose that the longitude of the central meridian of the map is λ_0; we then define

$$\ell = \frac{\lambda - \lambda_0}{180} \qquad -1 \leq \ell \leq 1$$

$$b = \frac{\phi}{180} \qquad -\tfrac{1}{2} \leq b \leq \tfrac{1}{2}$$

The longitude scale is linear along the equator. Meridians are arcs of circles passing through the appropriate point on the equator and both poles. Their radius r is given by

$$r = \rho \left(\ell + \frac{1}{\ell}\right) \qquad |r| \geq 2\rho$$

where the scale of the map is defined by the value assigned to ρ, which is the map distance corresponding to 90° of longitude along the equator. The center of the circle is along the equator at the point

$$x_M = \rho \left(\ell - \frac{1}{\ell}\right)$$

The last two equations can be combined to give

$$r^2 = x_M^2 + 4\rho^2$$

Thus the ±180° meridians ($\ell = \pm 1$) define a circle of radius $r = 2\rho$. The 90° east meridian ($\ell = 0.5$) is the arc of a circle of radius $r = 2.5\rho$ centered at $x_M = -1.5\rho$ and crossing the equator at $x = \rho$.

PRECEDING PAGE BLANK NOT FILMED

The parallels are circles whose radius, s, is given by

$$s = \frac{2\rho \cos z}{\sin 2\alpha}$$

where z is defined by:

$$\sin z = \frac{b}{1 - |b|} \qquad -90° \leq z \leq 90°$$

$$\tan \alpha = \frac{\sin z - \tan \mu}{\cos z}$$

and

$$\sin 2\mu = 2b \qquad -45° \leq \mu \leq 45°$$

The parallels intersect the prime meridian at

$$y = 2\rho \tan \mu$$

Thus the center of the circle defining the parallel is at

$$y_J = s + 2\rho \tan \mu$$

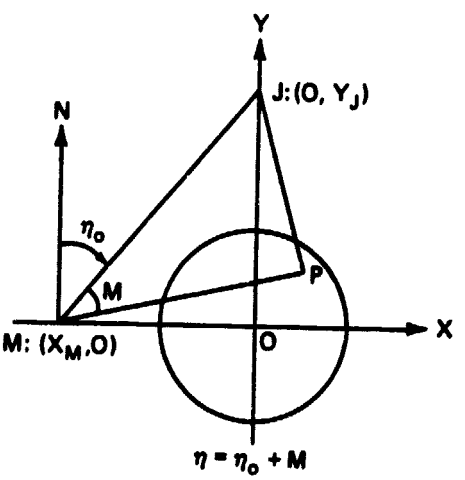
The geometry for the northeast quadrant is given in the attached figure. The x - y coordinates of the point P can be obtained by solving triangle MJP:

$MP = r$

$PJ = s$

$$JM = \Delta = \left(x_M^2 + y_J^2\right)^{1/2}$$

$$\tan \eta_o = -\frac{x_M}{y_J} \qquad 0 \leq \eta \leq 2\pi$$



The angle M is defined by

$$s^2 = r^2 + \Delta^2 - 2r\Delta \cos M$$

Then

$$x = r \sin \eta + x_M$$

$$y = r \cos \eta.$$

where

$$\eta = \eta_o + M$$

The geometry and formulas for the other three quadrants are given in the O'Keefe and Greenberg paper.

ORTHOGRAPHIC PROJECTION

The orthographic polar projection used in Plates 12, 13, 18, and 19 shows the earth's hemisphere as it would appear if viewed from infinity. In polar coordinates:

$$r = \rho \cos \phi$$

$$\theta = \lambda$$

for the North polar cap, where ϕ and λ are latitude and longitude and the scale factor ρ, true only at the center of the projection, is the map distance corresponding to $180/\pi$ degrees of latitude. The sign of θ is reversed for the south pole.

REFERENCES

Van der Grinten, A. J., New circular projection of the whole earth's surface, *Am. Jour. Sci., 19,* 357-366, 1905.

O'Keefe, J. A., and A. Greenberg, A note on the Van der Grinten projection of the whole earth onto a circular disk, *Amer. Cartographer, 4,* 127-132, 1977.

VAN DER GRINTEN GRID

ORIGINAL PAGE IS
OF POOR QUALITY

SECTION 2: SATELLITE-DERIVED GRAVITY MAPS

James G. Marsh

INTRODUCTION

Mapping the earth's gravity field and determining its shape (the geoid) were among the first major scientific applications of data from artificial satellites. As early as 1958, a new value for the flattening of the earth was derived from the tracking of Sputnik II. Since then, progressively more detailed models of the earth's gravity field and the geoid (or equipotential surface) have been constructed, based on hundreds of thousands of measurements of satellite orbits. We present here maps constructed from the latest of these, the Goddard Earth Model 10 (GEM 10).

A helpful review of the use of satellite data in mapping the earth's gravity field has been published by King-Hele (1976). The general subject of the earth's shape and gravity field is covered by, for example, Garland (1965).

DATA SOURCES AND COMPILATION METHODS

The GEM 10 (Lerch, et al., 1977) is the latest in a series of models developed by Goddard Space Flight Center. Even-numbered models ("combination solutions") are based on satellite and surface gravity data, odd-numbered models on satellite data alone. The GEM 10 model consists of a set of spherical harmonic coefficients complete to degree and order 22, with selected higher degree terms out to degree 30. It was derived from a combination of over 840,000 observations of 30 satellites, of which 200,000 are precision laser ranges on 9 satellites, and a global set of 1654 5°x 5° mean free-air surface gravity anomalies.

Three gravity anomaly maps are presented: one showing anomalies corresponding to the complete model, and two showing anomalies corresponding to degree and order 0–12 and 13–22. These maps are free-air anomaly maps, as contrasted with Bouguer maps. Among the major features shown by the full field map are: a major low south of India; a broad negative anomaly over the northwest Pacific; negative anomalies over Hudson Bay and Antarctica; positive anomalies over the Andes and Himalayas. The (0–12) map shows the long wavelength portion of the field. The India low is very prominent, and a positive ring clearly depicted around the Pacific basin closely matches plate boundaries. The (13–22) map is primarily characterized by features with half wavelengths of about 1000 km; some larger features shown on the (0–12) map have accordingly been removed. It has been postulated (Marsh and Marsh, 1976) that the anomalies shown on the (13–22) map in the eastern Pacific may be indicative of convective rolls beneath the Pacific plates. The Mid-Atlantic ridge and the hot spot locations show no characteristic anomaly patterns. However, a prominent positive anomaly is apparent along the east African rift system.

The fourth map presented here shows a detailed gravimetric geoid computed by combining the GEM 10 potential field model and a set of 38,406 1° x 1° mean free-air surface gravity anomalies. The long wavelength (~ 1500 km) undulations were calculated using the GEM 10 gravity model and the short wavelength components were computed by applying Stokes' formula to 1° x 1° mean residual anomalies. (The residual anomaly is the surface anomaly minus the satellite-derived anomaly.) Large geoidal lows (corresponding to negative gravity anomalies) are visible south of India, over Hudson Bay, and in the Pacific Ocean west of Baja California. Significant highs (corresponding to positive gravity anomalies) are visible over the Andes, south of Iceland, and over New Guinea.

REFERENCES

Garland, G. D., The Earth's Shape and Gravity, Pergamon Press, New York, 183 p., 1965.

King-Hele, D., The shape of the Earth, *Science, 192,* 1293–1300, 1976.

Lerch, F. G., S. M. Klosko, R. E. Laubscher, and C. A. Wagner, Gravity model improvement using GEOS-3 (GEM 9 and 10), X-921-77-246, Goddard Space Flight Center, Greenbelt, Md., 1977.

Marsh, B. D., and J. G. Marsh, On global gravity anomalies and two-scale mantle convection, *J. Geophys. Res., 81,* 5267-5280, 1976.

GRAVITY FIELD ANOMALIES

Full Field

Based on Goddard Earth Model - 10

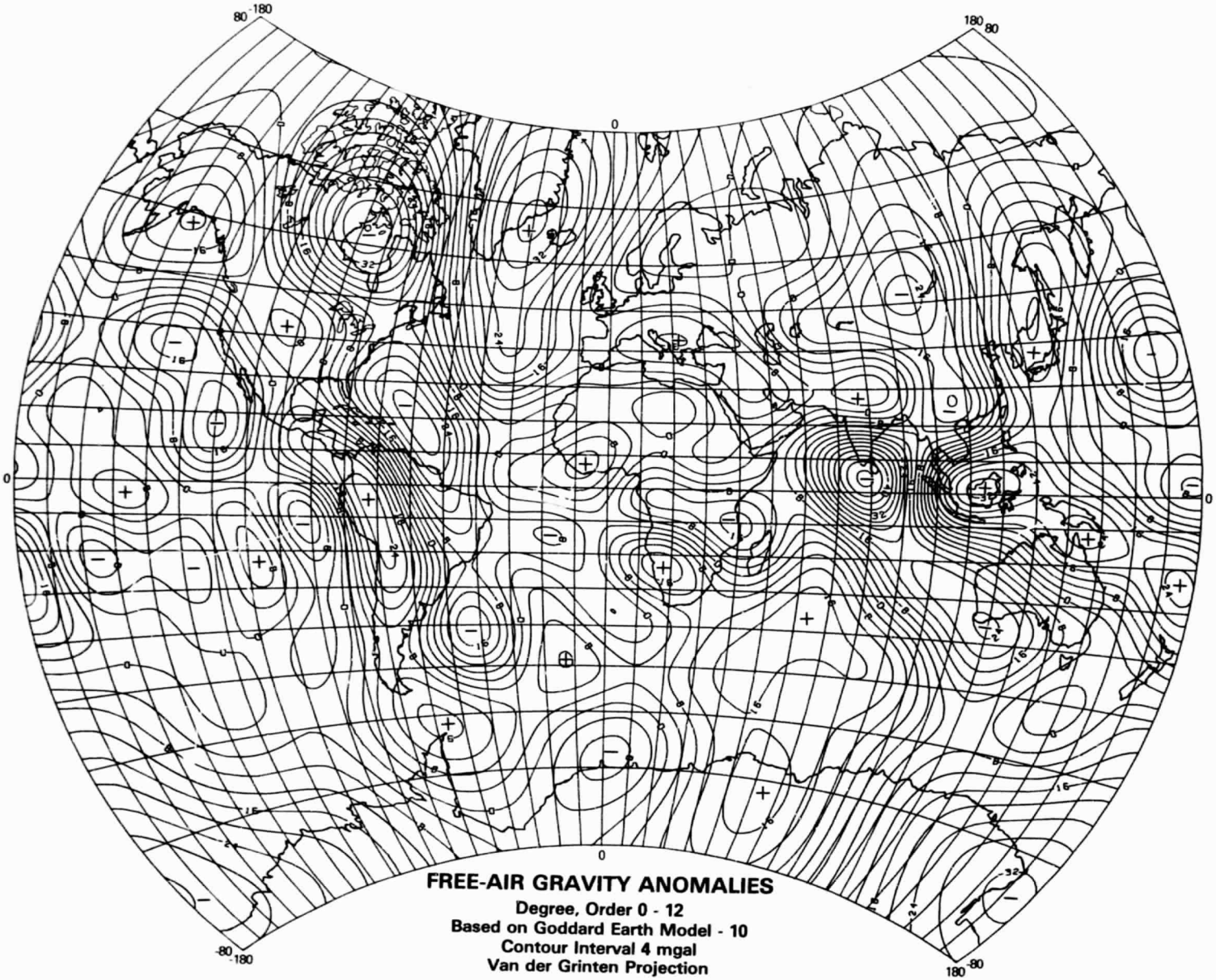
Contour Interval 4 mgal

Van der Grinten Projection

Goddard Space Flight Center

1978

ORIGINAL PAGE IS
OF POOR QUALITY



FREE-AIR GRAVITY ANOMALIES

Degree, Order 0 - 12
Based on Goddard Earth Model - 10
Contour Interval 4 mgal
Van der Grinten Projection

Goddard Space Flight Center

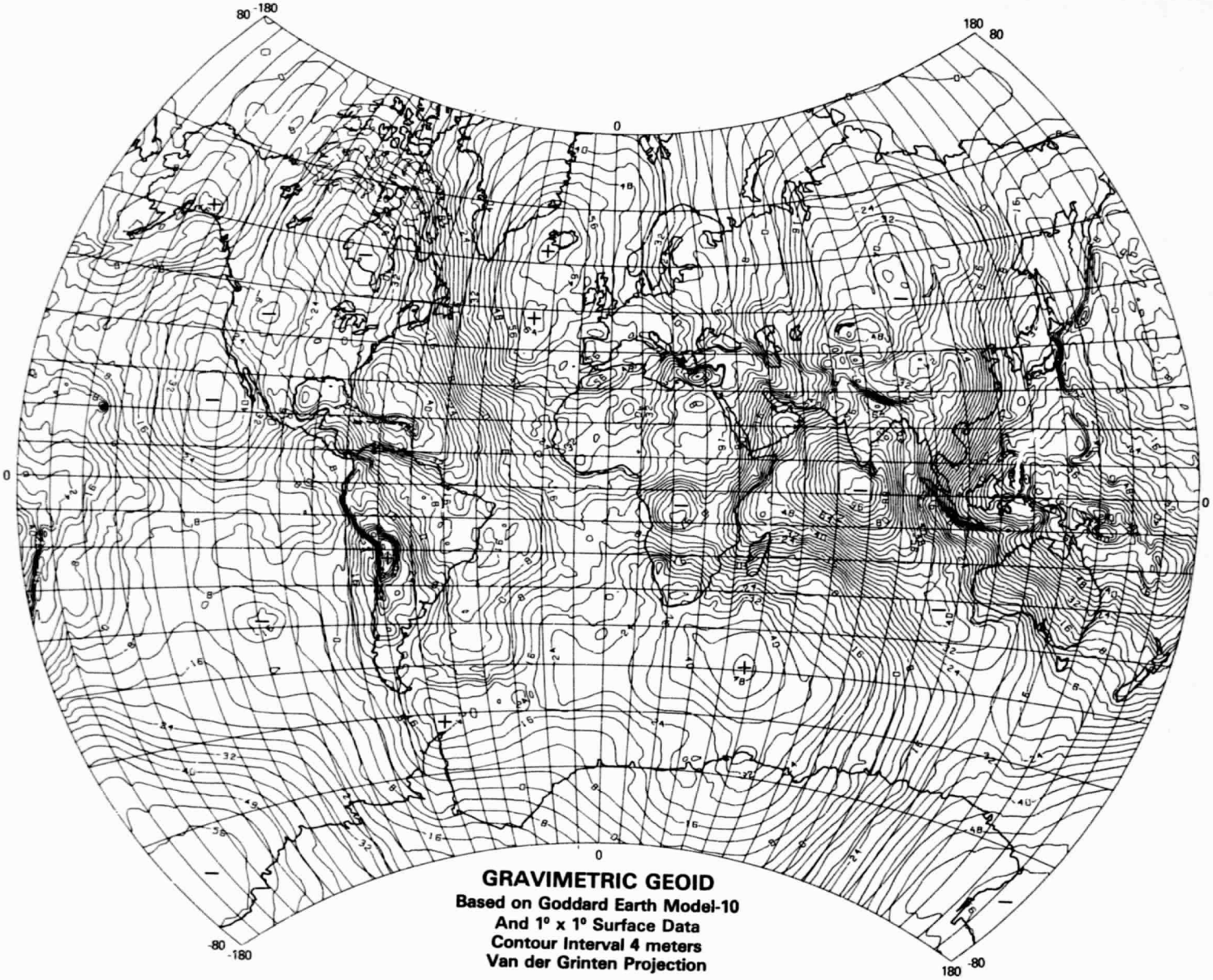
1978

FREE-AIR GRAVITY ANOMALIES
Degree, Order 13 - 22
Based on Goddard Earth Model - 10
Contour Interval 4 mgal
Van der Grinten Projection

Goddard Space Flight Center

1978

ORIGINAL PAGE IS
OF POOR QUALITY



GRAVIMETRIC GEOID
Based on Goddard Earth Model-10
And 1° x 1° Surface Data
Contour Interval 4 meters
Van der Grinten Projection

Goddard Space Flight Center

1978

SECTION 3: SATELLITE-DERIVED MAGNETIC ANOMALY MAPS

H. V. Frey, R. A. Langel, and W. M. Davis

INTRODUCTION

Although not intended for such applications, the magnetic field measurements made by the Polar Orbiting Geophysical Observatory satellites (POGO-2, 4, and 6) were used by Regan et al. (1975) to construct a map of global crustal magnetism in the mid-latitudes. This map, the first such ever produced, revealed many anomalies, several of which have been confirmed by ground or aerial surveys. We present here modified versions of this map.

DATA SOURCES AND COMPILATION METHODS

This presentation represents a slight modification and expansion of the data presented by Regan et al. (1975), and is shown as contoured residual values after removal of a 13th degree and order main field (or core field). Two data sets were used, one with geomagnetic latitude limits of ±60°, the other with geographic latitude limits of ±50°. All the data were derived from POGO observations during magnetically quiet periods, excluding measurements during local daylight to avoid external field changes. These have been further treated in two ways to eliminate the pronounced north-south orbital striping of the first map published by Regan et al. These treatments are outlined briefly as follows; further details can be found in Langel (1974).

Because typical signals measured at satellite altitudes (400-1500 km for the POGO series) are comparable in strength to those due to time variations in external field sources (e.g., ionospheric currents), these external sources must be removed from the data to determine the anomaly field due to internal sources. Contributions from distant external sources (above the ionosphere) and from long wavelength ionospheric sources can be modeled to first order by the low order terms in a spherical harmonic expansion (Langel and Sweeney, 1971; Cain and Davis, 1973). At middle geomagnetic latitudes (<60°) the effects of fields introduced by ionospheric currents can be minimized by excluding data from 0900 to 1550 local time. Restriction to <60° geomagnetic latitude also reduces contributions from polar and auroral zones. If these corrections successfully remove the effects of external fields, the remaining signals are due to the Earth's main field (i.e., the core field) and whatever lithospheric sources exist. The main field was modeled by Regan et al. by a 13th degree and order spherical harmonic expansion. Residuals from this field model are presumed to result from magnetic sources in the upper lithosphere.

Despite the corrections described, the original POGO map showed strong north-south striping in the residuals, clearly related to the satellite orbital paths. Two approaches have been used to eliminate these distracting and spurious features, both based on 2° block averages rather than the 1° averages used by Regan et al. This coarser average represents very well the observed anomalies with little loss of spatial resolution.

The first and simplest approach adopted was to further average out the orbital striping effects (which introduce high frequency noise along east-west lines) after removal of the external source model described above. Each value within a 2° block was adjusted by taking a weighted average with its nearest eight neighboring points; i.e., the data were smoothed in two dimensions using a nine-point weighted average. This clearly dampens the high-frequency noise introduced by the incomplete removal of the long wavelength magnetospheric currents, and results in what will be referred to as a "smoothed" anomaly map.

The second approach was based on Mayhew's (1977) study of individual POGO passes over the United States. Using a subset of the data with similar orbital altitudes, Mayhew found that individual profiles over the same region were not identical after correction for external effects. A long-wavelength residual remained in what should have been identical profiles; this was partly responsible for the north-south striping in the original map. Mayhew found that an internally consistent data set could be produced by fitting linear or quadratic functions through the individual residual profiles, and used that data set to generate an equivalent source representation of the anomaly field over the United States. This approach has been adopted here and applied to individual passes before the 2° averaging; the resulting plot will be referred to as a "filtered" anomaly map.

Both approaches have shortcomings, and neither explicitly identifies the nature of the noise responsible for the striping. There are differences between the maps generated by the two techniques, which are particularly obvious for long wavelength features. In general, the "smoothing" procedure has probably failed to completely remove spurious external fields (e.g., magnetospheric effects), while the Mayhew filtering procedure may have removed these but in addition some of the lithospheric field features.

Three anomaly maps are presented. The first (Plate 7), a smoothed anomaly map, represents 2° block averages contoured at 2 gamma intervals between 60° geomagnetic latitude limits. This data set is slightly expanded over that used by Regan et al. (1975). The second map (Plate 8), a smoothed version,is similar to the first, but the anomalies are patterned with vertical and horizontal stripes reflecting the intensity of the anomalies. The zero contour has been eliminated for clarity. As in the first map, the contour interval is 2 gammas, but anomalies with absolute intensity greater than 6 gammas are shown only by 6 gamma stripes. The density of stripes in the pattern shows intensity of the anomalies, with horizontal stripes representing negative anomalies and vertical ones positive anomalies. This format readily displays the anomalies without the use of a color code such as that used by Regan et al.

The third map (Plate 9) shows a filtered version of the anomaly data (patterned). This map is limited to <50° geographic latitude to accommodate restrictions in the Mayhew filtering technique. It is clear that most anomalies display only slight differences. However, there are some obvious changes, notably the anomalies in the Pacific west of Peru and Chile, in South Africa, and near Madagascar. Similar discrepancies for a small fraction of the anomalies occur if the quadratic filter recommended by Mayhew (1977) is used instead of the linear trend removed here.

REFERENCES

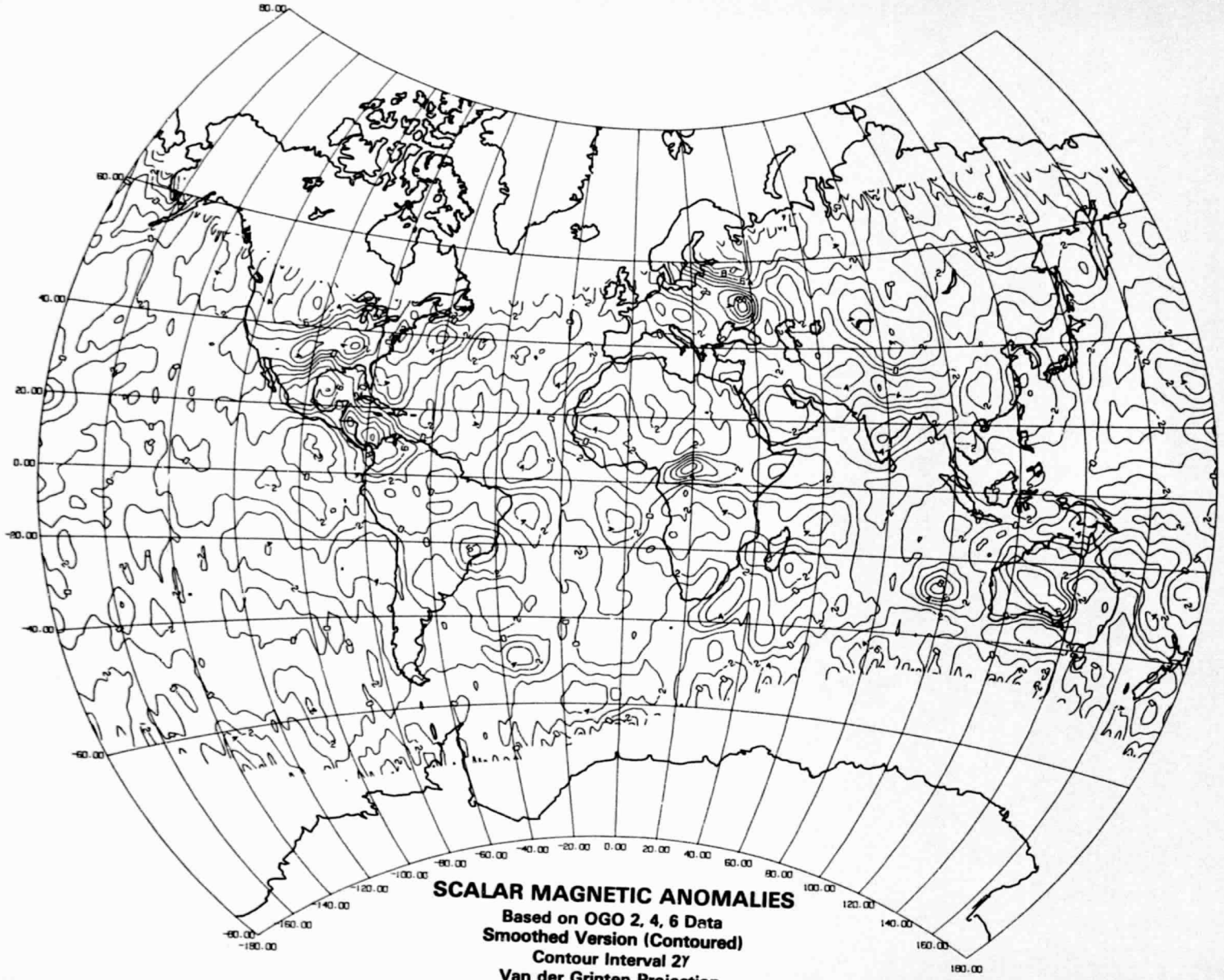
Cain, J. C., and W. M. Davis, Low latitude variations of the magnetic field, in Symposium on Low-level Satellite Surveys, International Association of Geomagnetism and Aeronomy, Paris, 1973.

Langel, R. A., Near-Earth magnetic disturbance in total field at high latitudes: summary of data from OGO 2, 4, and 6, *J. Geophys. Res.*, *79*, 2363-2371, 1974.

Langel, R. A., and R. E. Sweeney, Asymmetric ring current at twilight local time, *J. Geophys. Res.*, *76*, 4420-4427, 1971.

Mayhew, M. A., A method of inversion of satellite magnetic anomaly data, X-922-77-260, Goddard Space Flight Center, Greenbelt, Md., 17 p., 1977.

Regan, R. D., J. C. Cain, and W. M. Davis, A global magnetic anomaly map, *J. Geophys. Res.*, *80*, 794-802, 1975.



SCALAR MAGNETIC ANOMALIES

Based on OGO 2, 4, 6 Data
Smoothed Version (Contoured)
Contour Interval 2γ
Van der Grinten Projection

Goddard Space Flight Center

1978

ORIGINAL PAGE IS
OF POOR QUALITY

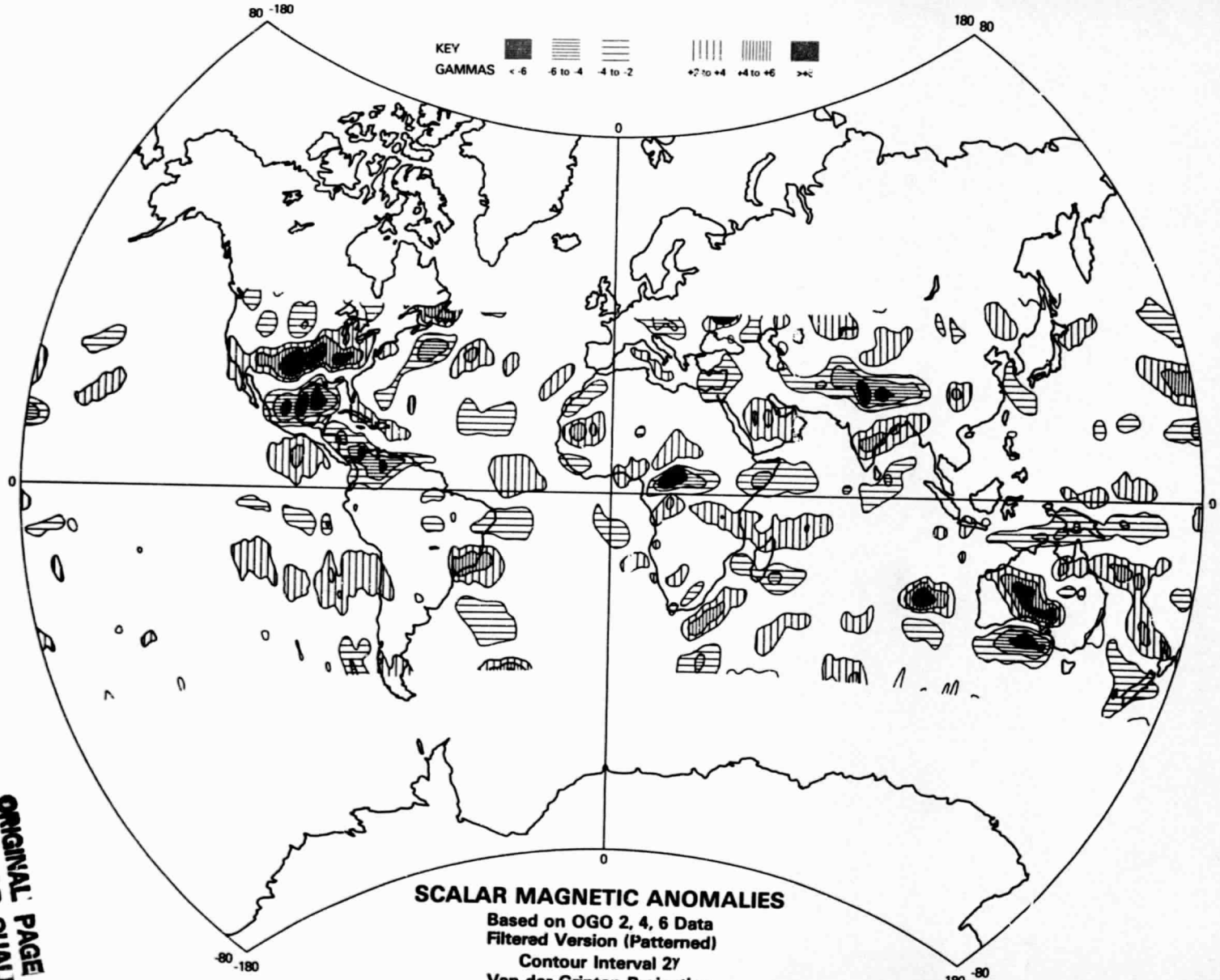
SCALAR MAGNETIC ANOMALIES

Based on OGO 2, 4, 6 Data
Smoothed Version (Patterned)
Contour Interval 2γ
Van der Grinten Projection

Goddard Space Flight Center

1978

ORIGINAL PAGE IS
OF POOR QUALITY



SCALAR MAGNETIC ANOMALIES

Based on OGO 2, 4, 6 Data
Filtered Version (Patterned)
Contour Interval 2γ
Van der Grinten Projection

Goddard Space Flight Center

1978

ORIGINAL PAGE IS
OF POOR QUALITY

SECTION 4: GLOBAL SEISMICITY MAPS

M. K. Hutchinson
P. D. Lowman

A series of four maps (Plates 10-13) showing the global distribution of earthquakes has been compiled to serve as a guide in depicting tectonic activity. Two of the maps show seismic epicenters between ±80° latitude: one with continental outlines, the other without. In addition, we have compiled maps of the north and south polar regions, down to 40° latitude, to provide global coverage. Each map can be compared directly with a corresponding tectonic activity map in this atlas.

DATA SOURCES AND COMPILATION METHODS

All the seismicity maps are computer plots derived from a data tape supplied by the National Geophysical and Solar-Terrestrial Data Center (NOAA) in Boulder, CO. This tape includes information such as data source, time of origin, location to three decimal places, focal depth, and associated phenomena if relevant. Seismic and other data tapes available from NOAA are described in Report SE-14, published by World Data Center A for Solid Earth Geophysics, National Oceanic and Atmospheric Administration, Boulder, CO 80303.

The period 1965-75 was chosen for plotting primarily because events from this period were recorded by the World Wide Network of Standardized Seismographic Stations (WWNSSS) established in the early 1960's. These data are more accurate than those from earlier times. Computer limitations restricted the number of data points that could be plotted, and the magnitude interval 4.5 to 5.5 (generally M_L) was therefore chosen. As the maps demonstrate, despite the narrowness of this interval, earthquakes of this magnitude are quite numerous enough to outline zones and specific features of tectonic activity. One reason for this is that events larger than magnitude 5.5 have many aftershocks of lower magnitude. No discrimination was made on the basis of depth, with all earthquakes down to 700 kilometers being plotted. Intermediate and deep focus events are abundant in subduction zones such as the Peru-Chile trench; outside such zones, almost all earthquakes are shallow-focus (0-70 km depth); (Tarr, 1974).

The map without continental outlines (Plate 10) includes 27,000 epicenters. Because of computer limitations, the inclusion of continental outlines required reduction in the number of points plotted; Plate 11 thus includes only 16,000 epicenters. To insure accurate delineation of seismic features, the reduction was accomplished by plotting the first 10 events in each 2° block, so that the net cartographic effect was simply a decrease in point density in the most active and best-defined seismic areas.

These maps give a reasonably true and complete picture of the distribution of present seismic activity over the whole earth. Areas of little or no apparent seismicity in particular are probably areas in which tectonic activity at this time actually is minor. Antarctica is especially conspicuous in this regard; the near-absence of earthquakes from this continent is definitely not an effect of instrument placement, seismometers having been operating there for some two decades.

The distribution of seismic activity along the oceanic ridges also deserves some comment. First, it is obvious that the activity varies drastically both along individual ridges and between ridges. What is not obvious is that the fastest spreading centers, in particular the East Pacific Rise, are not the most active ridges; seismicity apparently is greater along the Mid-Atlantic Ridge, whose spreading rate is much lower than that of the East Pacific Rise. Whether this is an artifact resulting from the

PRECEDING PAGE BLANK NOT FILMED

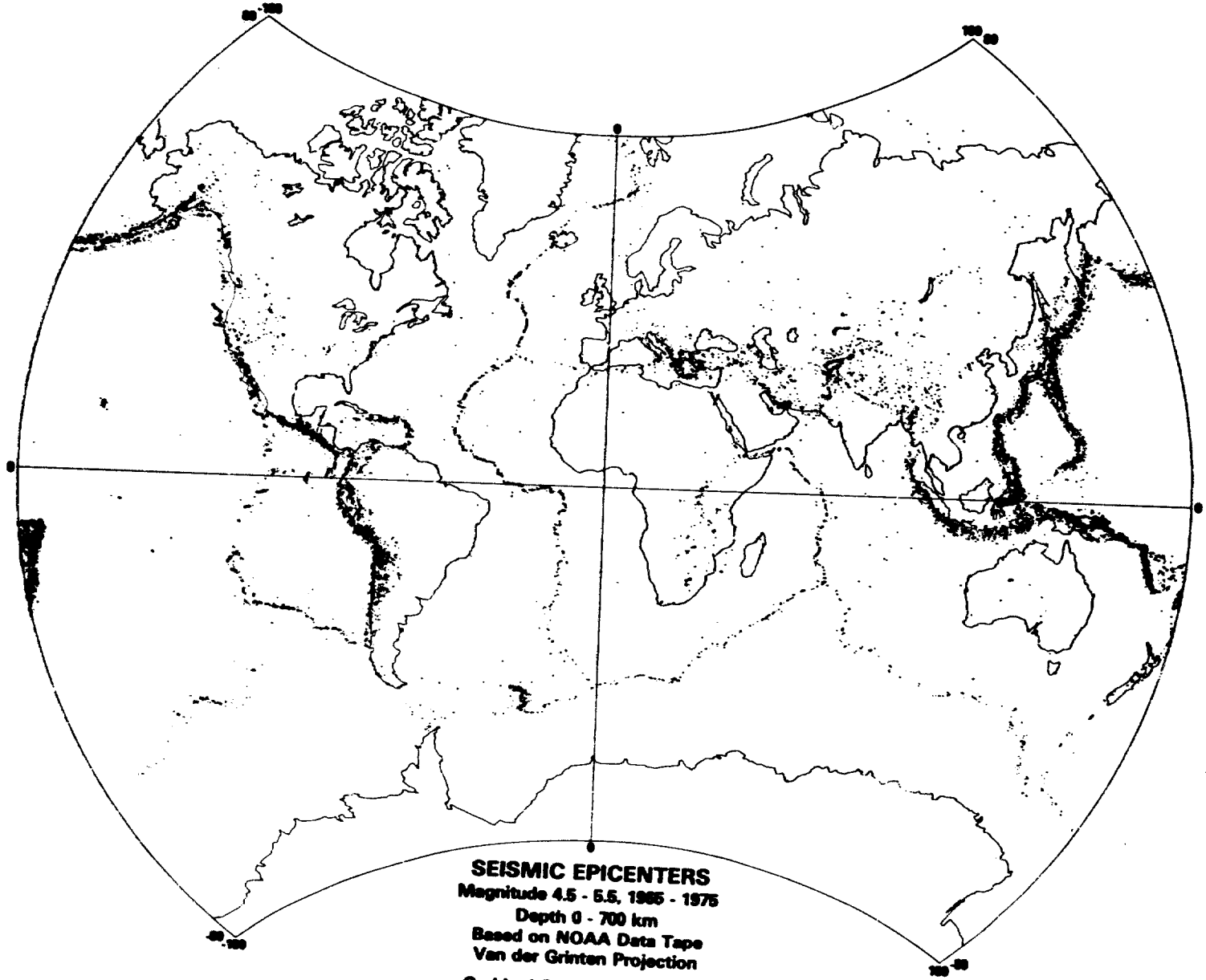
shortness of the instrumental record, the narrow time interval plotted, or a real phenomenon, deserves study.

One effect of the short time period represented by these maps, discussed at length by Allen (1976), is that some major faults known to be active are unrecognizable on the seismicity plots. For example, the South Atlas fault bounding the Atlas Mountains, which was responsible for the earthquake that nearly destroyed the city of Agadir in 1961, exhibits only one event in the 1965-75 period. These maps by themselves thus do not for many areas give an accurate index of seismic risk or of tectonic activity. The maps of tectonic and volcanic activity presented elsewhere in this atlas (Plates 17-19) were therefore based on many criteria in addition to the seismicity maps.

REFERENCES

Allen, C. R., Geological criteria for evaluating seismicity, *Bull. Geol. Soc. Amer.*, *86*, 1041-1057, 1975.

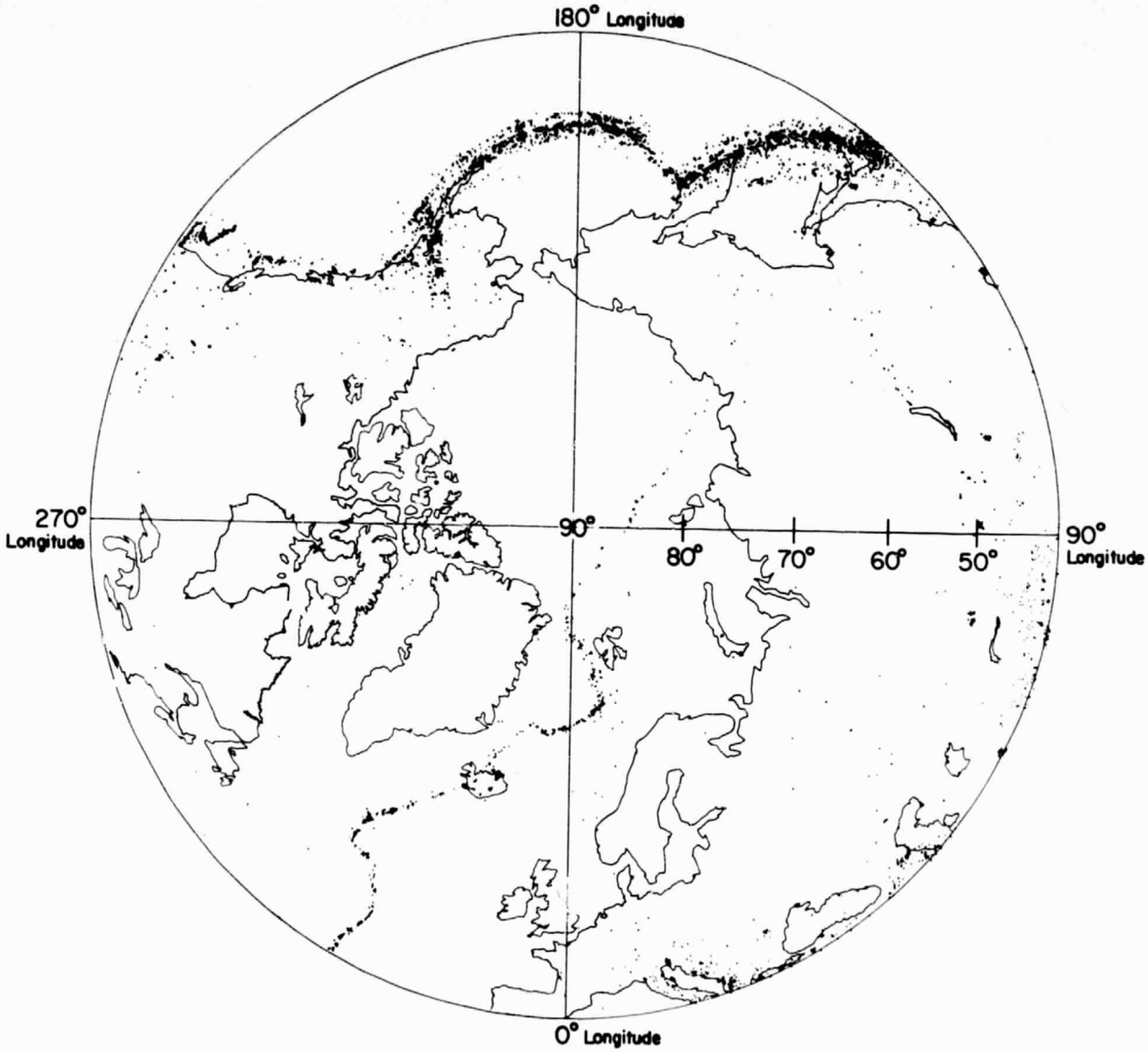
ORIGINAL PAGE IS
OF POOR QUALITY



SEISMIC EPICENTERS
Magnitude 4.5 - 5.5, 1965 - 1975
Depth 0 - 700 km
Based on NOAA Data Tape
Van der Grinten Projection

Goddard Space Flight Center

1976



ARCTIC SEISMICITY

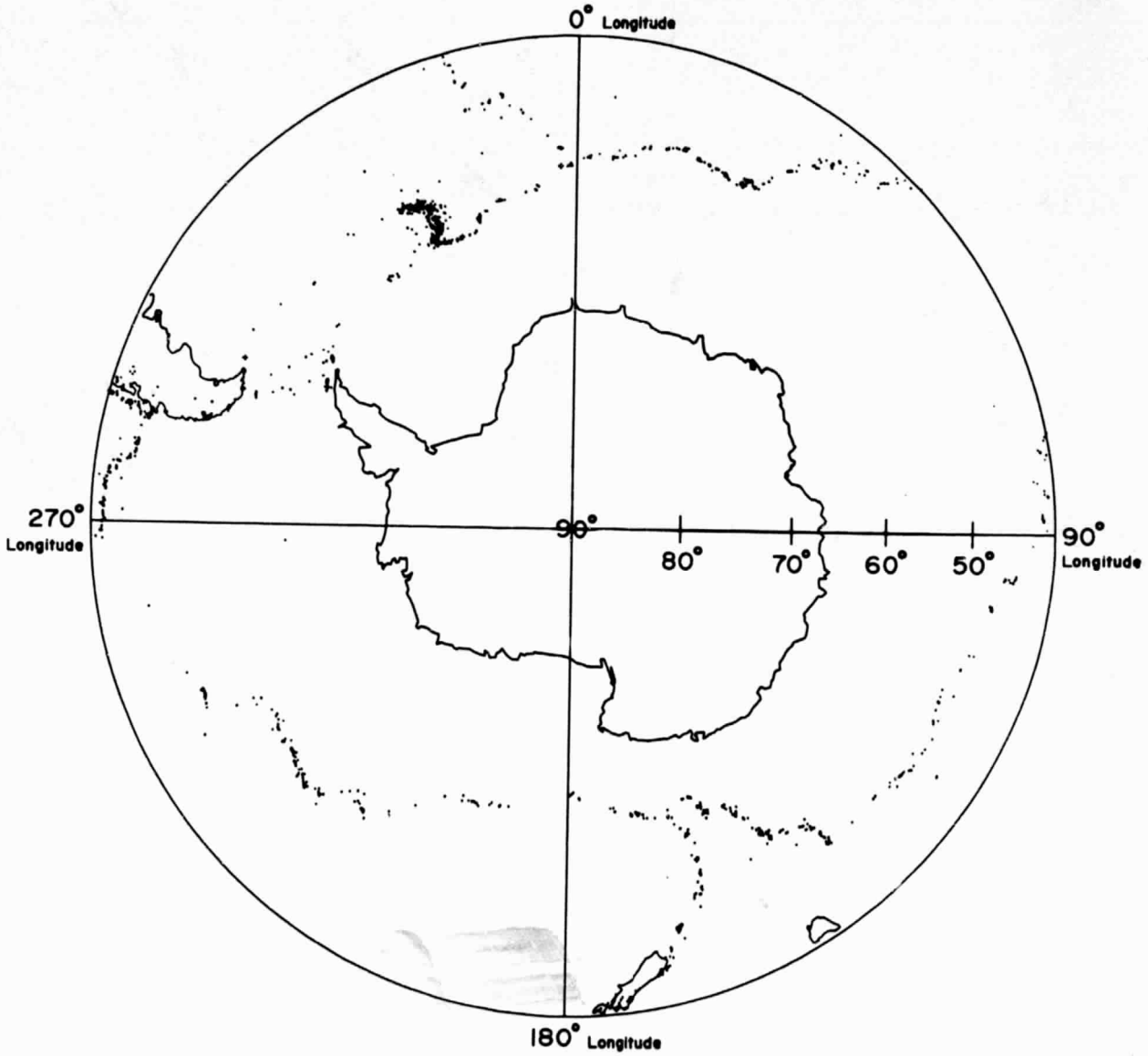
Epicenters of 4,518 Earthquakes, 1965-75
M.4.5 - 6.9 (•), > 7.0 (+), 0-700 km Depth
Based on NOAA Data Tape

Orthographic Projection
40° to 90° Latitude

Compiled 1978

Goddard Space Flight Center

ORIGINAL PAGE IS
OF POOR QUALITY



ANTARCTIC SEISMICITY

Epicenters of 1,136 Earthquakes, 1965-75
M.4.5 - 6.9 (•), > 7.0 (+), 0-700 km Depth
Based on NOAA Data Tape

Orthographic Projection
40° to 90° Latitude

Compiled 1978

Goddard Space Flight Center

SECTION 5: RECENT VOLCANIC ACTIVITY MAP

Aron P. Trombka
Paul D. Lowman

This computer-plotted map (Plate 14) displays the geographical distribution of recent volcanic centers. Both currently-active volcanic centers and those active within the last one million years are included.

DATA SOURCES AND COMPILATION METHODS

The major reference for active volcanoes was the Catalogue of Active Volcanoes of the World by the International Association of Volcanology. Older volcanic centers were identified by using geologic and tectonic maps, especially those published by various national surveys. Recent information used to supplement outdated maps included the articles "Makran of Iran and Pakistan as an Active Arc System" by G. Farhoudi and D. E. Karig and "Concealed Mesozoic-Cenozoic Alpine Himalayan Geosyncline and its Petroleum Possibilities" by S. K. Acharrya and K. K. Ray. For some isolated structures Landsat images were used to locate the features.

The symbol (+) on the map represents one of these features:

- All volcanic activity (central or fissure) listed as currently active by the International Association of Volcanology or by other sources.
- Any activity recorded (and confirmed by consulting a geologic map) during historical time.
- An uneroded structure listed as "volcano" (A physical structure, e.g., a volcanic cone, that remains intact is probably less than one million years old, and as such is included here if the geology of the region, as indicated on a geologic map, supports the presence of young volcanic material).
- Lava or tephra fields definitely dated as formed within the past one million years.
- Submarine volcanoes found within tectonic plates (hot spots) or those that form volcanic islands; however, all submarine volcanic activity associated with the mid-oceanic ridges and seafloor spreading has been omitted from this map.

Any individual (+) indicates only the geographical point corresponding to the volcanic center and not the eruptive history of that center, i.e., repetitive activity from the same feature is plotted as a single (+).

MAP LIMITATIONS

Although this map is a complete compilation of all known active volcanoes, information for other features is less complete. Volcanic features other than volcanoes (e.g., solfatara fields, geysers), even while currently active, are in many instances never documented.

Inactive volcanic centers present additional difficulties. Exact dating of volcanic features becomes important when using such a brief time frame of one million years. Most of the younger

inactive volcanic centers have prominent physical characteristics such as a caldera, but the older centers with ages slightly less than one million years may be indistinguishable from volcanism of two or three million years. This map includes only those centers definitely dated as active within one million years and so is probably incomplete. In some cases where the exact location of older volcanic centers within a volcanic field is questionable the symbol (+) is plotted at the probable location; this serves as an adequate representation on a map of this scale, with the greatest discrepancy being approximately three-quarters of a degree.

Submarine volcanism is itself a fairly recent discovery and there is little available documentation of specific events. Therefore, only a few submarine volcanoes (other than those associated with sea-floor spreading at mid-oceanic ridges) have been dated as active within the last one million years. For both submarine and continental cases, reported but unconfirmed activity has been omitted from this map.

REFERENCES

Acharrya, S. K., and K. K. Ray, Concealed Mesozoic-Cenozoic Alpine Himalayan Geosyncline and its Petroleum Possibilities, *Amer. Assoc. Petroleum Geologists Bull.*, V. 60, No. 5, pp. 794-808, 1976.

Adie, R. J., *Antarctic Geology: Proceedings of the First International Symposium of Antarctic Geology*, J. Wiley and Sons, Inc., New York, 758 p., 1964.

Bandrabur, T., C. Ghenea, M. Sandulescu, and M. Stefanescu, Republica Socialista Romania; Harta Neotectonica (Map), 1:1,000,000, Institutului Geologic, Bucharest, 1971.

Bartholomew, J., The Times Atlas of the World; Mid-Century Ed. Houghton Mifflin Co., Boston, 1958.

Bullard, F. M., Volcanoes in History, in Theory, in Eruption, University of Texas Press, Austin, pp. 95-404, 1962.

Clifford, T. N., and I. G. Gass, African Magmatism and Tectonics, Hafner Pub. Co., Darien, Conn., pp. 185-210, 263-283, 301-319, 1970.

Farhoudi, G., and D. E. Karig, Makran of Iran and Pakistan as an Active Arc System, *Geology*, V. 5, No. 11, pp. 664-668, 1977.

Green, J., and N. Short, Volcanic Landforms and Surface Features: A Photographic Atlas and Glossary, Springer-Verlag, New York, 519 p., 1971.

Grim, P. J., Terrestrial Heat Flow (Map), World Data Center A, Boulder, CO., 1976.

Grosvenor, M. B., National Geographic Atlas of the World, Revised Third Ed., National Geographic Soc., Washington, DC, 1970.

Gutenberg, R., and C. F. Richter, Seismicity of the Earth and Associated Phenomena, Princeton Univ. Press, Princeton, NJ, 273 p., 1949.

Holmes, A., 1965, Principles of Physical Geology, Second Ed., Ronald Press, New York, 1288 p., 1965.

International Association of Volcanology, 1951-1967, Catalogue of the Active Volcanoes of the World Including Solfatara Fields, Vols. 1-21, Naples, Rome, Italy.

Instituto Geographico Militar, Ecuador (Map), 1:1,000,000, Quito, Ecuador, 1974.

King, P. B., and G. J. Edmonston, Generalized Tectonic Map of North America, 1:15,000,000, Map I-688, U.S. Geological Survey, 1972.

Lowman, P. D., The Third Planet: Terrestrial Geology in Orbital Photographs, Weltflugbild, Zurich, 170 p., 1972.

Lowman, P. D., Global Tectonic Activity (Map), Goddard Space Flight Center, Greenbelt, MD, 1978.

Pesce, A., Gemini Space Photographs of Libya and Tibesti: A Geological and Geographical Analyses, Petroleum Exploration Soc. of Libya, Tripoli, 82 p., 1968.

Rittmann, A., Volcanoes and their Activity, J. Wiley and Sons, New York, pp. 153-157, 1962.

Rutten, M. G., The Geology of Western Europe, Elsevier Pub. Co., Amsterdam, pp. 432-469, 1969.

Wilson, J. T., and K. C. Burke, Hot Spots on the Earth's Surface, *Sci. Amer.*, V. 235, pp. 46-56, 1976.

Yanskin, A. L., Tectonic Map of Asia, 1:5,000,000, USSR Ministry of Geology, Moscow, 1966.

ORIGINAL PAGE IS
OF POOR QUALITY

SECTION 6: TECTONIC BOUNDARIES: RIFT AND SUTURE MAPS

Herbert V. Frey

INTRODUCTION

The two maps (Plates 15 and 16) presented here were constructed by the Albany Global Tectonics Group* under the direction of Kevin Burke (Chairman, Department of Geology, State University of New York at Albany). They are the only ones intended to show major tectonic elements as such. It is appropriate to include specialized tectonic maps to aid correlative study of the satellite-derived geophysical data, although it is not obvious just what types of maps will be most helpful. Rifts and sutures are major tectonic elements representing, in plate tectonic theory, the opening and closing, respectively, of ocean basins, and they may delineate boundaries of lithospheric properties. Maps of these structures thus represent a necessary first step for the incorporation of plate tectonic data in the Atlas.

DATA SOURCES AND COMPILATION METHODS

The criteria used to identify rifts and sutures are those adopted by The Albany Global Tectonics Group, as specified in several publications (Burke, 1977; Burke et al., 1977; Dewey, 1977). In addition, the maps are described and documented in a contractor report, "Rifts and Sutures of the World," available from Goddard Space Flight Center, which funded their preparation under NASA contract NAS 5-24094.

"Rifts," as shown here, are extensional ruptures penetrating a substantial thickness of the lithosphere. As such, they represent major boundaries in lithospheric properties. This is especially true for the continental rifts, which are the only ones preserved that are older than about 200 million years (the oceanic rifts are eventually destroyed by plate movements). Perhaps the best known intra-continental rift system is that in East Africa, which includes the type Gregory rift. Other well-known systems include the Lake Baikal rift, the Oslo and Rhine grabens, and the Rio Grande rift. These and lesser-known rifts are mapped and described in the above-named contractor report.

Not all rifts develop into active spreading centers, and except for those now active (see the tectonic activity map), the rifts shown on this map must be those which failed or whose development was arrested before developing into a continental margin. Some features displayed here are aulacogens: fault-bounded troughs with thick sedimentary sequences striking at high angles into fold belts (Burke, 1977). These may be rifts that failed, were subsequently filled with sediments and modified by continental collisions.

The natural consequence of plate tectonic theory is that continental blocks and other tectonic elements should collide. Complete closure of an ocean through subduction of the oceanic lithosphere stops when continental margins come into contact. The buoyancy of continental crust prevents its destruction through subduction. The weld where two previously-separated continental blocks join is often called, in plate tectonic theory, a suture. Sutures are seldom lines, but more often wide and complex zones displaying a variety of high-strain structures (Dewey, 1977). Ideally,

*The Albany Global Tectonics Group includes Kevin Burke, Louise Delano, J. F. Dewey, A. Edelstein, W. S. F. Kidd, K. D. Nelson, A. M. C. Sengor, and J. Stroup.

they are marked by ophiolite sequences consisting of basic and ultrabasic rocks considered by many to represent slices of oceanic crust mechanically emplaced during the continental collision (Dewey, 1977). Ophiolites are in this concept the evidence for closure of an ocean. Because ophiolites may not, however, always be present, and because a variety of processes and topographic landforms are involved in convergent tectonics, the criteria used to identify paleo-sutures are somewhat less rigorous than those available in the case of rifts. Dewey (1977) and Burke et al. (1977) describe some of the properties and characteristics used. The map presented here is an updated version of the "World Distribution of Sutures" previously published (Burke et al., 1977). The basic thesis of these authors is that Precambrian plate tectonics produced numerous ocean openings and closings, and that old fold belts and other structures overlie the site of closure of ancient ocean basins.

The two maps presented here have both been coded by ages of the rifts or sutures. Details are presented in the above-described contractor report. The restriction to black and white required the use of symbols whose clarity is sometimes questionable. Alternative formats are being considered, and may be used in future versions of this Atlas.

REFERENCES

Burke, K., Aulacogens and continental breakup, *Ann. Rev. Earth Planet Sci., 5*, 371-396, 1977.

Burke, K., J. F. Dewey, and W. S. F. Kidd, World distribution of sutures - the sites of former oceans, *Tectonophysics, 40*, 69-99, 1977.

Dewey, J. F., Suture zone complexities: a review, *Tectonophysics, 40*, 53-67, 1977.

ORIGINAL PAGE IS
OF POOR QUALITY

ORIGINAL PAGE IS
OF POOR QUALITY

SECTION 7: GLOBAL TECTONIC AND VOLCANIC ACTIVITY MAPS

Paul D. Lowman, Jr.

These maps are intended to show the geographic distribution of major tectonic and volcanic activity at the present time and for approximately the past one million years. There are three overlapping maps, for the equatorial, Arctic, and Antarctic regions, which can serve as base maps for the qualitative interpretation of satellite data shown on other sheets of the Atlas.

COMPILATION METHODS AND DATA SOURCES

The equatorial tectonic activity map was drawn as an overlay on a 1:72,700,000 scale copy of the National Geographic Society's "The Physical World" (1975). The actual delineation of tectonic and volcanic features was generally a compromise among several different representations, including published maps and papers listed in the bibliography. Plate boundaries, where well-defined, were drawn primarily from the epicenter patterns as plotted on the maps of global seismicity. Features included on the maps are described below.

FEATURES DISPLAYED

Active Ridges

This category includes centers of sea-floor spreading and related continental rift zones. Activity is inferred from seismicity, but there is insufficient information in some areas to determine if apparently inactive ridge segments have been active within the past million years. An example of this problem is the segment of the East Pacific Rise at about 40°S, 110°W. Transform faults offsetting oceanic ridges are highly generalized. Large oceanic fracture zones prominent on most maps, such as those of the eastern Pacific, are not shown here because they are now understood to be the inactive traces of transform faults.

Subduction or Overthrust Zones

Subduction and overthrust zones are both essentially reverse faults (though frequently associated with fold belts), and they have accordingly been grouped together. This grouping may reflect a genetic relationship in many areas, such as the Himalayas, which are thought to represent a continent-continent subduction zone quite analogous to and continuous with the Java trench. Subduction zones have been located on the map over trenches representing their intersection with the surface of the earth. A strike-slip component of movement near subduction zones is shown only where prominent, as in the fold belts of Burma and Pakistan.

Major Active Faults

This is a broad category for faults exhibiting good evidence (seismic or physiographic) of present or recent movement. Physiographic criteria, such as fresh scarps, were used by several authors whose work has been drawn upon, to infer fault activity; as pointed out by Allen (1975), such criteria are more reliable than the historic record of seismicity. Whether physiographic evidence of faulting necessarily indicates activity within the past one million years (the criterion for inclusion on this map) is an open question which is beyond the scope of this discussion; the reader is referred to literature cited for individual structures.

Rifts or Zones of Normal Faulting

This category includes areas of well-documented extensional tectonism not necessarily related to oceanic spreading centers. These features have been highly generalized in many areas, and some individual rifts have been shown with exaggerated widths for clarity. Fault-controlled valleys of the Basin and Range province are shown only schematically, since it was impossible to represent them all at this scale.

Young Volcanoes

This category includes chiefly volcanic areas of the central eruptive type, although a few (notably Iceland) have associated fissure eruptions. The problem of whether a volcano now inactive has erupted within the past one million years is for many areas a difficult one. It is obvious that this map and the "Recent Volcanic Activity" map (Plate 14) include many more volcanoes than those generally catalogued as "active," though omitting many features shown as hot spots by Burke and Wilson (1976) (whose age cut-off was 10 million years). Inclusion in the one million year age category was largely on the basis of physiography. It appears, from study of the published literature (e.g., Hopkins, 1963) , that volcanoes in general survive as identifiable land forms for roughly a million years; i.e., if a feature is labeled "volcano" on a reliable map it is probably no older than this.

It should be noted that active oceanic ridges are also the sites of igneous activity, although this is not shown explicitly on the map except for a few major volcanic centers such as Iceland.

Unresolved Problems

As a service to the user, some of the weaknesses of this map should be pointed out. A fundamental inconsistency occurs between the seismicity and tectonic activity maps, in that a number of areas exhibiting seismicity are not represented on the tectonic activity map; examples include the Appalachians, the Urals, and the Canadian Arctic islands. This omission was caused by the difficulty of assigning the seismicity patterns to discrete tectonic features. In some areas, particularly the Appalachians, seismic activity may result from reactivation of Paleozoic structures. The problem will be addressed in future editions of the Atlas.

A related problem is the treatment of "passive" continental margins, such as those of the Atlantic Ocean. The actual degree of activity over the last million years is quite unknown, and there is growing evidence of Tertiary or Quaternary deformation, for example, along the margin of eastern North America (Mixon and Newell, 1977) and of strong regional stress in this area (Sbar and Sykes, 1973). This problem is a fundamental one whose solution must await more information about the nature of these features.

DISCUSSION

These tectonic activity maps fill a cartographic gap between conventional geologic maps and maps showing present seismic and volcanic activity. Although based partly on compilations of current activity, the use of geologic evidence of recent age permits extrapolation back about one million years, giving a much more comprehensive view of global tectonic and volcanic activity. An example of this is furnished by the many volcanic areas shown in the Alpine fold belt, very few of which are included in conventional compilations. Although most of these volcanoes are not now active, they are obviously related to the Alpine orogeny.

The tectonic activity maps show most of the generally recognized tectonic plates and related features. However, they also show many structures generally omitted from conventional plate maps

such as that of Le Pichon et al. (1972), especially active structures located within plates or diffuse plate boundaries. Examples of these include the faults of western China, the Basin and Range province, and the strike-slip faults of Alaska. Omission of such features can obscure important relationships, such as the fundamental symmetry of the Alpine fold belt in the Middle East discussed by Holmes (1965).

In summary, the tectonic activity maps presented here provide a more realistic picture of crustal dynamic processes on a global basis than do conventional maps. They should be useful for geophysical correlations as well as for tectonic research and education.

REFERENCES

Albany Global Tectonic Group, Rifts and Sutures of the World, NASA Contract Report NAS5-24094, Goddard Space Flight Center, Greenbelt, Md., 238 p., 1978.

Allen, C. R., Geological criteria for evaluating seismicity, *Geol. Soc. America Bull., v. 86,* p. 1041-1057, 1975.

American Geographical Society, The Floor of the Oceans (based on studies by B. C. Heezen and M. Tharp), 1:40,000,000 equatorial scale, American Geographical Society, New York, N.Y. 10032, 1974.

Anderson, R. N., M. G. Langseth, and J. G. Sclater, The mechanisms of heat transfer through the floor of the Indian Ocean, *J. Geophys. Res., v. 82,* p. 3391-3409, 1977.

Atwater, T., Implications of plate tectonics for the Cenozoic tectonic evolution of western North America, *Geol. Soc. America Bull., v. 81,* p. 3513-3536, 1970.

Ben Avraham, Z., and A. Nur, Slip rates and morphology of continental collision belts, *Geology, 4,* 661-664, 1976.

Barker, P. F., A spreading centre in the East Scotia Sea, *Earth and Planet. Sci. Lett., 15,* 123-132, 1972.

Bergh, H. W., and I. O. Norton, Prince Edward fracture zone and the evolution of the Mozambique Basin, *J. Geophys. Res., v. 81,* p. 5221, 1976.

Burke, K. C., and J. T. Wilson, Hot spots on the Earth's surface, *Sci. American, 235,* 46-57, August 1976.

Chesser, W. L., and W. K. Hamblin, Physiographic Map of the Earth, Burgess Pub. Co., Minneapolis, Minn., 1975.

Churkin, M., Jr., Western boundary of the North American continental plate in Asia, *Geol. Soc. America Bull., v. 83,* p. 1027-1036, 1972.

Dalziel, I. W. D., Evolution of the margins of the Scotia Sea, in The Geology of Continental Margins, edited by C. A. Burk and C. L. Drake, pp. 567-569, Springer-Verlag, New York, 1009 p., 1974.

Dewey, J. F., Plate tectonics, *Sci. American, 226,* 56-68, 1972.

Dewey, J. F., and J. M. Bird, Mountain belts and the new global tectonics, *Jour. Geophys. Res., v. 75,* p. 2625-2647, 1970.

Dewey, J. F., W. C. Pitman, III, W. B. F. Ryan, and J. Bonnin, Plate tectonics and the evolution of the Alpine System, *Geol. Soc. America Bull., v. 84,* p. 3137-3180, 1973.

Forsyth, D. W., Fault plane solutions and tectonics of the South Atlantic and Scotia Sea, *J. Geophys. Res., 80,* 1429-1443, 1975.

Gansser, A., Geology of the Himalayas, Interscience Publishers, New York, 289 p., 1964.

Gutenberg, B., and C. F. Richter, Seismicity of the Earth and Associated Phenomena, Princeton University Press, Princeton, NJ, 273 p., 1949.

Hilde, T. W. C., S. Uyeda, and L. Kroenke, Tectonic history of the western Pacific, in Geodynamics: Progress and Prospects, edited by C. L. Drake, pp. 1-15, Am. Geophys. Union, Washington, DC, 238 p., 1976.

Hinze, W. J., L. W. Braile, G. R. Keller, and E. G. Lidiak, A tectonic overview of the central midcontinent (preprint) 98 p., 1977.

Holmes, A., Principles of Physical Geology, Second Edition, Ronald Press, New York, 1288 p., 1965.

Hopkins, D. M., Geology of the Imruk Lake area, Seward Peninsula, Alaska, U.S. Geological Survey Bulletin 1141-C, Contributions to General Geology in 1961, 1963.

Isaacks, B., J. Oliver, and L. R. Sykes, Seismology and the new global tectonics, *J. Geophys. Res., 73,* 5855-5899, 1968.

Johnson, G. L., and P. R. Vogt, Marine geology of Atlantic Ocean north of the Arctic Circle, in Arctic Geology, edited by M. G. Pitcher, Mem. 19, pp. 161-170, Am. Assoc. Petroleum Geologists, Tulsa, Oklahoma, 747 p., 1973.

Kaula, W. M., Global gravity and tectonics, in The Nature of the Solid Earth, edited by E. C. Robertson, J. F. Hays, and L. Knopoff, pp. 385-405, McGraw-Hill, New York, 677 p., 1972.

King, P. B., and G. J. Edmonston, Generalized Tectonic Map of North America, 1:15,000,000: Map I-688, U.S. Geological Survey, Reston, Va., 1972.

Kirkham, R. M. Quaternary movements on the Golden fault, Colorado, *Geology, 5,* 689-692, 1977.

Lathram, E. H., Nimbus IV view of the major structural features of Alaska, *Science, 175,* 1423-1427, 1972.

Le Pichon, X., J. Francheteau, and J. Bonnin, Plate Tectonics, Elsevier, New York, 300 p., 1973.

Lowman, P. D., Jr., The Third Planet, Weltflugbild, Zurich, Switzerland, 185 p., 1972.

McKenzie, D. P., Speculations on the consequences and causes of plate motions, *Geophys. Jour. Royal Astronomical Soc., 18,* 1-32, 1969.

McKenzie, D. P., and W. J. Morgan, Evolution of triple junctions, *Nature, 224,* 125-133, 1969.

Meyerhoff, A. A., Origin of Arctic and North Atlantic Oceans, in Arctic Geology, edited by M. G. Pitcher, Mem. 19, pp. 562-583, Am. Assoc. Petroleum Geologists, Tulsa, Oklahoma, 747 p., 1973.

Mixon, R. B., and W. L. Newell, Stafford fault system: structures documenting Cretaceous and Tertiary deformation along the fall line in northeastern Virginia, *Geology, 5,* 437-440, 1977.

Molnar, P., and P. Tapponier, Relation of the tectonics of eastern China to the India-Eurasia collision: application of slip-line field theory to large-scale continental tectonics, *Geology, 5,* 212-216, 1977.

Muehlberger, W. R., and A. W. Ritchie, Caribbean-Americas plate boundary in Guatemala and southern Mexico as seen on Skylab IV orbital photography, *Geology, 3,* 232-235, 1975.

O'Keefe, J. A., and A. Greenberg, A Note on the Van der Grinten Projection of the Whole Earth Onto a Circular Disk, *The American Cartographer, v. 4,* no. 2, p. 127-132, 1977.

Powell, C. McA., and P. J. Conaghan, Tectonic models of the Tibetan plateau, *Geology, 3,* 727-731, 1975.

Prostka, H. J., and S. S. Oriel, Genetic models for Snake River plain, Idaho (abstract), Abstracts With Programs, 1975 Annual Meeting, Geol. Soc. America, v. 7, no. 7, p. 1236, 1975.

Ray, K. K., and S. K. Acharyya, Concealed Mesozoic-Cenozoic Alpine-Himalayas geosyncline and its petroleum possibilities, *Am. Assoc. Petroleum Geologists Bull., 60,* 794-808, 1976.

Rutten, M. G., The Geology of Western Europe, Elsevier, New York, 520 p., 1969.

Sbar, M. L., and L. R. Sykes, Contemporary compressive stress and seismicity in eastern North America: an example of intra-plate tectonics, *Geol. Soc. Amer. Bull., 84,* 1861-1882, 1973.

Sclater, J. G., C. Bowin, R. Hey, H. Hoskins, J. Peirce, J. Phillips, and C. Tapscott, The Bouvet triple junction, *J. Geophys. Res., 81,* 1857-1869, 1976.

Simpson, R. W., and A. Cox, Paleomagnetic evidence for tectonic rotation of the Oregon Coast Range, *Geology, 5,* 585-589, 1977.

Smith, P. S., Mineral resources of the Lake Clark-Iditarod region, in Mineral Resources of Alaska: Reports on Progress of Investigations in 1914, edited by A. H. Brooks, pp. 247-271, U.S. Geological Syrvey Bulletin 622, 1915.

Stein, S., and E. A. Okal, Seismicity and tectonics of the Ninetyeast Ridge area: evidence for internal deformation of the Indian plate, *J. Geophys. Res., 83,* 2233-2245, 1978.

Swiss Reinsurance Company, Atlas on Seismicity and Volcanism, Kummerly-Frey Pub. Co., Zurich, 40 p., 1978.

Tapponier, P., and P. Molnar, Active faulting and tectonics in China, *J. Geophys. Res., 82,* 2905-2930, 1977.

White, R. S., and K. Klitgord, Sediment deformation and plate tectonics in the Gulf of Oman, *Earth and Planet. Sci. Lett., 32,* 199-209, 1976.

ORIGINAL PAGE IS
OF POOR QUALITY

ORIGINAL PAGE IS
OF POOR QUALITY

GLOBAL TECTONIC AND VOLCANIC ACTIVITY
OF THE LAST ONE MILLION YEARS

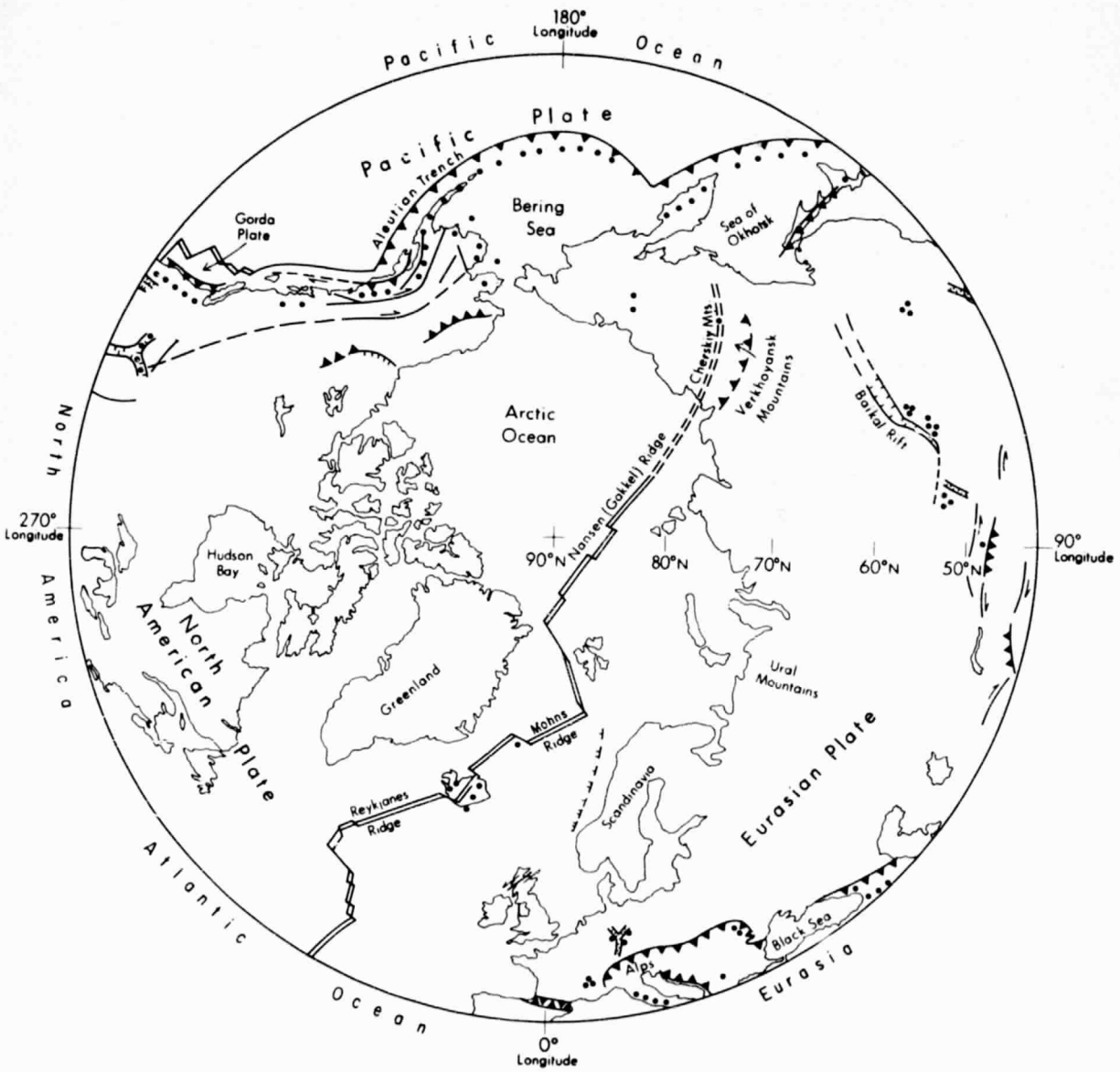
Goddard Space Flight Center
1978

Based on "The Physical World," copyright 1975 by the National Geographic Society.
Van der Grinten Projection.

Paul D. Lowman Jr.

LEGEND

- Active ridges and continental extensions; minor faults generalized
- Subduction or overthrust zone; teeth on upper block
- Major active fault or fault zone; dashed where nature or activity uncertain
- Rift or zone of normal faulting; teeth on downthrown block
- Young volcanos (active within last 1 million years; generalized)



TECTONIC AND VOLCANIC ACTIVITY OF THE ARCTIC REGIONS
(Last one million years)
Goddard Space Flight Center
1978

Orthographic
Projection Covering
Latitudes 40° to 90° North

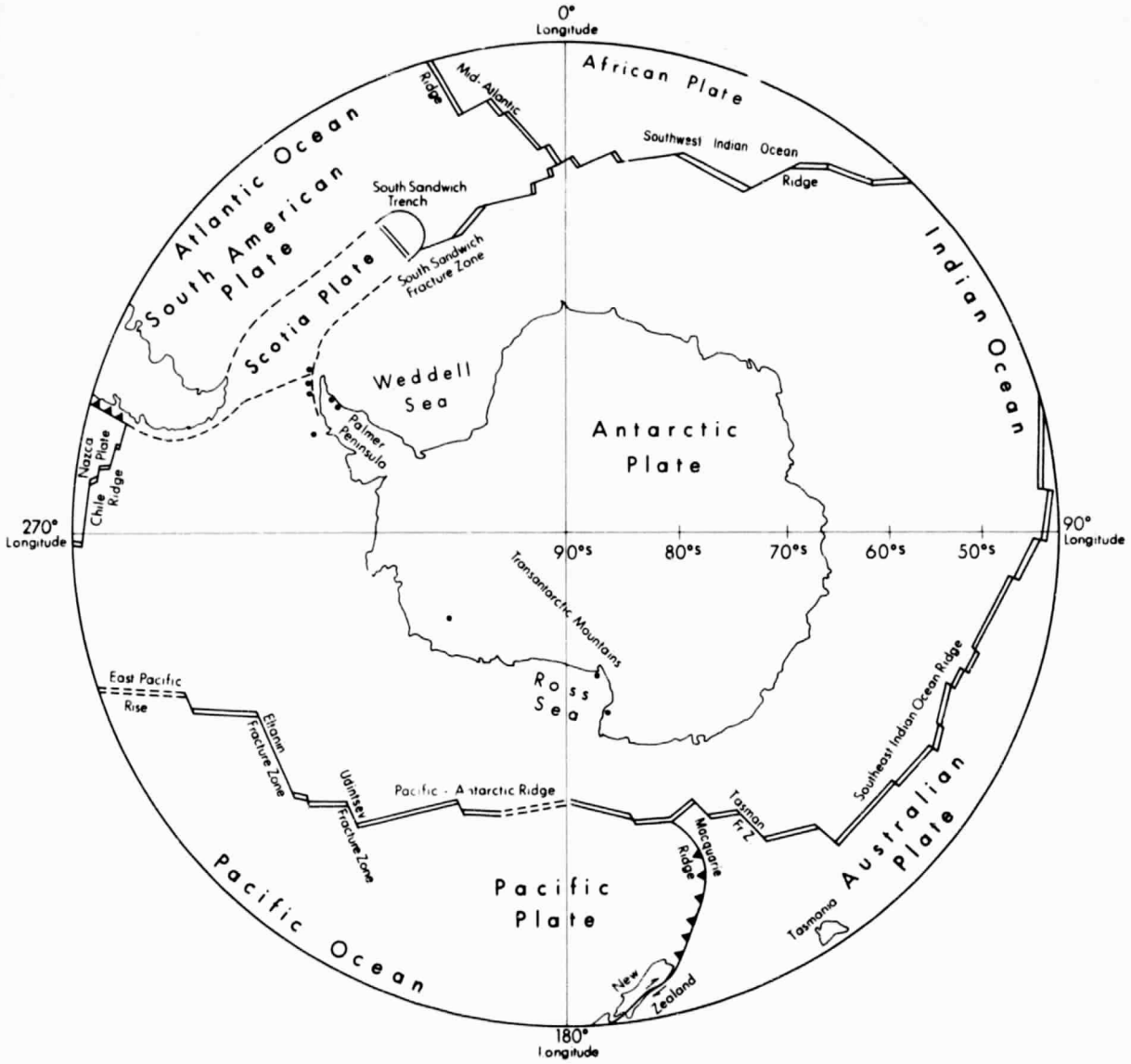
Polar Scale

1100 Km (10°)
680 Miles

LEGEND

- Active ridges and continental extensions, minor faults generalized
- Subduction or overthrust zone, teeth on upper block
- Major active fault, dashed where nature or activity uncertain
- Rift or zone of normal faulting, teeth on downthrown block
- Young volcanos (active within last 1 million years, generalized)

ORIGINAL PAGE IS
OF POOR QUALITY



TECTONIC AND VOLCANIC ACTIVITY OF THE ANTARCTIC REGIONS
(Last one million years)
Goddard Space Flight Center
1978

Orthographic
Projection Covering
Latitudes 40° to 90° South

Polar Scale

1100 Km (10°)
680 Miles

LEGEND

- Active ridges and continental extensions, minor faults generalized
- Subduction or overthrust zone, teeth on upper block
- Major active fault, dashed where nature or activity uncertain
- Rift or zone of normal faulting, teeth on downthrown block
- Young volcanos (active within last 1 million years, generalized)

ORIGINAL PAGE IS
OF POOR QUALITY

SECTION 8: SEISMIC VELOCITY ANOMALY MAPS

Barbara E. Lowrey

Long wavelength gravity anomalies such as those shown in Plate 4 reflect the mass distribution, or variation in density, in the deep interior of the Earth. To aid in understanding the causes of gravity anomalies, we have constructed a series of maps (Plates 20-29) showing anomalies in the velocities of seismic P-waves.

The velocity of seismic waves has for many years been a primary source of information on the structure of the earth's interior. Seismic wave travel times have been employed by many workers to determine the radial variation of density within the earth, assuming a spherically symmetric earth. However, it has for some time been recognized that there are lateral heterogeneities in the mantle. A major investigation has been undertaken by Dziewonski, Hager, and O'Connell (1977) to determine the feasibility of recovering the lateral velocity variations, i.e., the heterogeneities, in the mantle on a global basis by computing the differences between observed P-wave travel times and the standard Jeffreys-Bullen travel time tables. Dziewonski et al. constructed a spherical harmonic expansion of the velocity anomalies, and published a series of Mercator projection maps showing the anomalies in successively deeper shells.

Because the conversion of the recovered data into spherical harmonics truncated at degree and order 3 may lose numerical information, we have constructed contour maps directly from the recovered data, using the Van der Grinten projection common to the maps of this Atlas.

DATA SOURCES AND COMPILATION METHODS

The work of Dziewonski et al. was based on 12,882 earthquakes for the years 1964-1970 published in the Bulletin of the International Seismological Centre. Compression wave (P and PKP) times were used, being the most accurate and numerous. Residuals were computed by differencing the observed travel times with the Jeffreys-Bullen travel time tables. The mantle was divided into five concentric shells, with depths of 0-670, 670-1100, 1100-1500, 1500-2200, and 2200-2886 kilometers, and 36° wide latitudinal and 60° wide longitudinal zones. Two cases were investigated, the second involving rotation of meridional boundaries 30° to the west to see if the results had been biased by the longitudinal boundaries selected.

Dziewonski et al. reported that their results were unreliable for depths less than 1100 km, probably because lateral heterogeneities in this shell are generally smaller than 5000 km in lateral dimensions. However, they found a statistically significant correlation between long wavelength gravity anomalies observed at the surface and those computed from velocity anomalies deeper than 1100 km, assuming a proportionality between velocity and density perturbations. Their interpretation of these results will not be repeated here.

In the paper by Dziewonski et al., contour plots were constructed after several steps of numerical processing. First, spherical harmonic coefficients were computed according to two methods, numerical integration and least squares solution. Thus four sets of coefficients were computed for the two cases by two methods. The coefficients from the two cases were then combined for the two methods. Contours were constructed for each of the two methods and plotted together for comparison.

The contours on our maps were constructed for the two cases directly from the original data (velocity anomalies) tabulated by Dziewonski, without additional numerical treatment. This has

several advantages: (1) loss of information by truncation of the spherical harmonics is avoided, (2) uncertainties due to lack of data or poor resolution are mapped directly, rather than as artifacts elsewhere on the map, and (3) the tendency of spherical harmonics to produce non-existent anomalies is avoided. The method of contouring the original data is also useful in assessing the validity and degree of knowledge of a feature. Since the original study used large blocks (60° x 60°) to discretize the data, the geographic resolution of the data is about 30°. By comparing maps of a given depth region for the two cases, the size and strength of individual features can be assessed. In the upper two regions, there is little similarity between maps for the two cases, i.e., it is difficult to identify features common to both cases, probably because the resolution of the data is too coarse. However, in the lower three regions, there is a strong correlation between the two cases, although features may be offset as much as 30° because of the spatial resolution.

Our treatment introduces a certain degree of complexity and ambiguity to interpretation of the data. However, it is clear that the general features of the maps by Dziewonski et al. were reproduced, at least for the deep regions of the mantle. Our maps are intended not to replace those of Dziewonski et al., but to complement them by contouring the original values, thus providing a better idea of data quality and distribution. In addition, qualitative correlation between deep mantle structure and that of the lithosphere should be facilitated by the use of a scale and projection common to other geophysical maps, particularly gravity, in this Atlas.

REFERENCES

Dziewonski, A. M., B. H. Hager, and R. J. O'Connell, Large-scale heterogeneities in the lower mantle, *J. Geophys. Res., 82,* 239-255, 1977.

SEISMIC VELOCITY ANOMALIES (m/s)

Case 1: Depths 0 to 670 km
Based on Data from Dziewonski,
Hager, and O'Connell
Van der Grinten Projection

B. E. Lowrey
F. T. Heuring

Goddard Space Flight Center

1978

ORIGINAL PAGE IS
OF POOR QUALITY

SEISMIC VELOCITY ANOMALIES (m/s)

Case 1: Depths 670 to 1100 km
Based on Data from Dziewonski,
Hager, and O'Connell
Van der Grinten Projection

B. E. Lowrey
F. T. Heuring

Goddard Space Flight Center

1978

ORIGINAL PAGE IS
OF POOR QUALITY

SEISMIC VELOCITY ANOMALIES (m/s)

Case 2: Depths 1100 to 1500 km
Based on Data from Dziewonski,
Hager, and O'Connell
Van der Grinten Projection

B. E. Lowrey
F. T. Heuring

Goddard Space Flight Center

1978

ORIGINAL PAGE IS
OF POOR QUALITY

SEISMIC VELOCITY ANOMALIES (m/s)

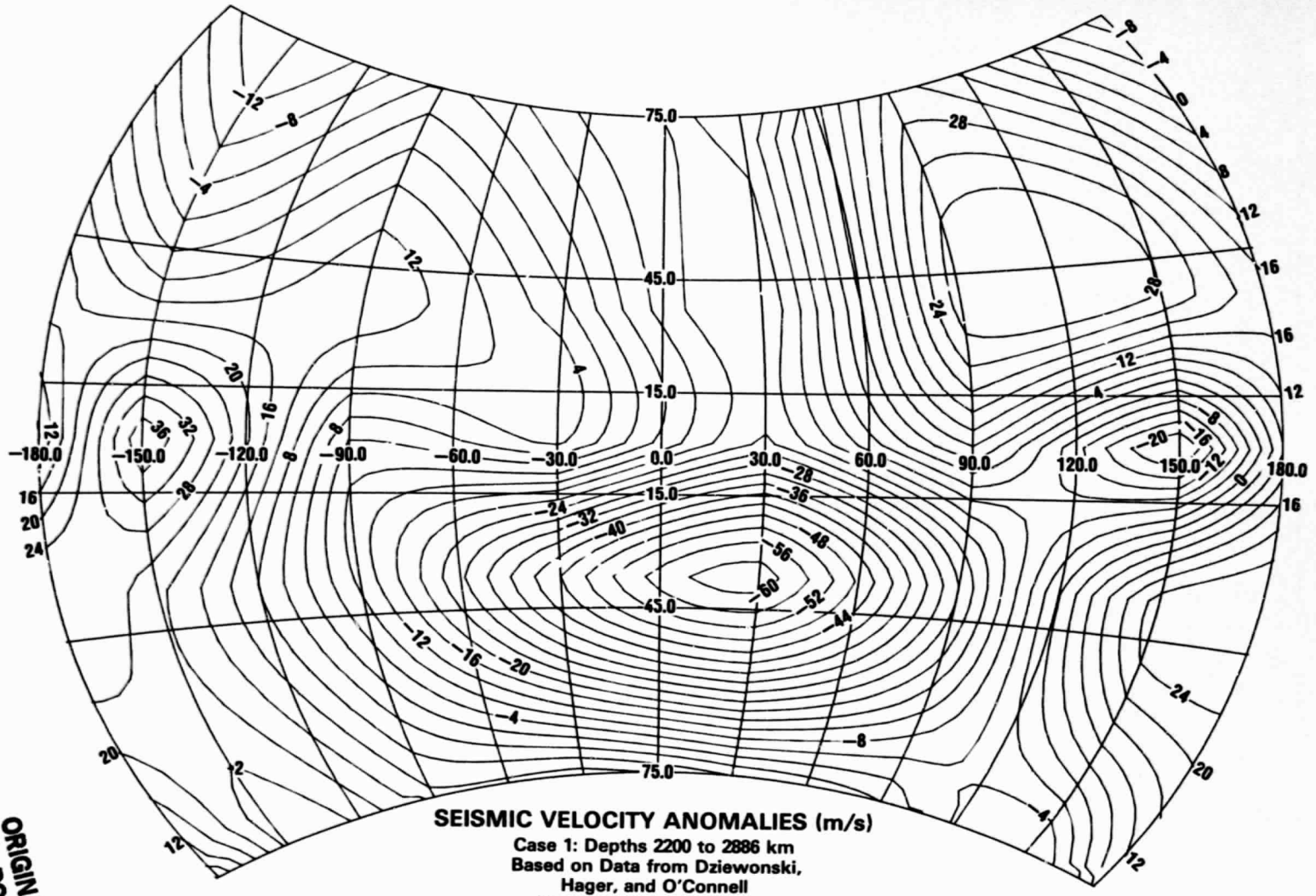
Case 1: Depths 1500 to 2200 km
Based on Data from Dziewonski,
Hager, and O'Connell
Van der Grinten Projection

B. E. Lowrey
F. T. Heuring

Goddard Space Flight Center

1978

ORIGINAL PAGE IS
OF POOR QUALITY



SEISMIC VELOCITY ANOMALIES (m/s)

Case 1: Depths 2200 to 2886 km
Based on Data from Dziewonski,
Hager, and O'Connell
Van der Grinten Projection

B. E. Lowrey
r. T. Heuring

Goddard Space Flight Center

1978

ORIGINAL PAGE IS
OF POOR QUALITY

SEISMIC VELOCITY ANOMALIES (m/s)

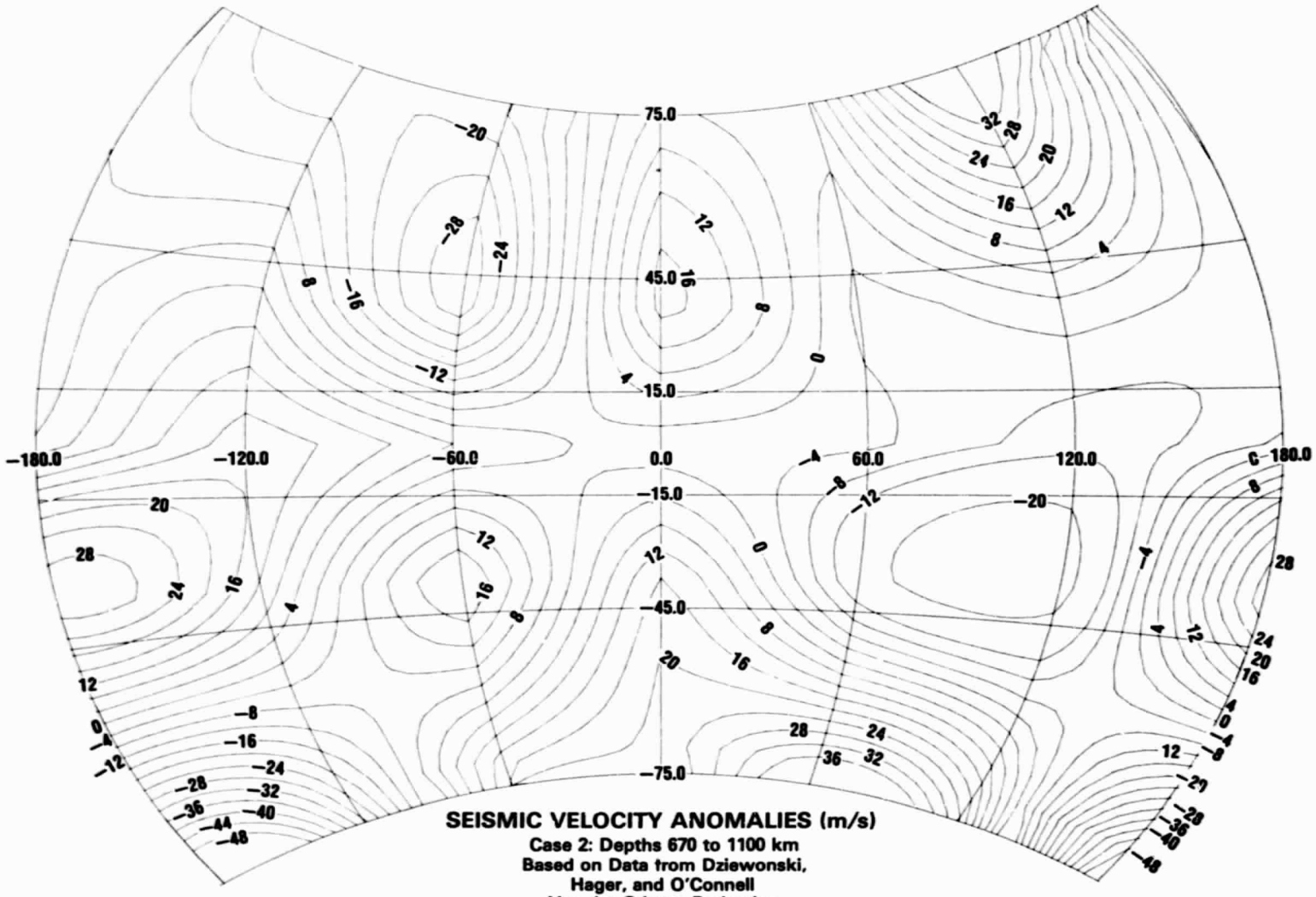
Case 2: Depths 0 to 670 km
Based on Data from Dziewonski,
Hager, and O'Connell
Van der Grinten Projection

B. E. Lowrey
F. T. Heuring

Goddard Space Flight Center

1978

ORIGINAL PAGE IS
OF POOR QUALITY



SEISMIC VELOCITY ANOMALIES (m/s)

Case 2: Depths 670 to 1100 km
Based on Data from Dziewonski, Hager, and O'Connell
Van der Grinten Projection

B. E. Lowrey
F. T. Heuring
Goddard Space Flight Center

1978

SEISMIC VELOCITY ANOMALIES (m/s)

Case 2: Depths 1100 to 1500 km
Based on Data from Dziewonski,
Hager, and O'Connell
Van der Grinten Projection

B. E. Lowrey
F. T. Heuring

Goddard Space Flight Center

1978

ORIGINAL PAGE IS
OF POOR QUALITY

SEISMIC VELOCITY ANOMALIES (m/s)

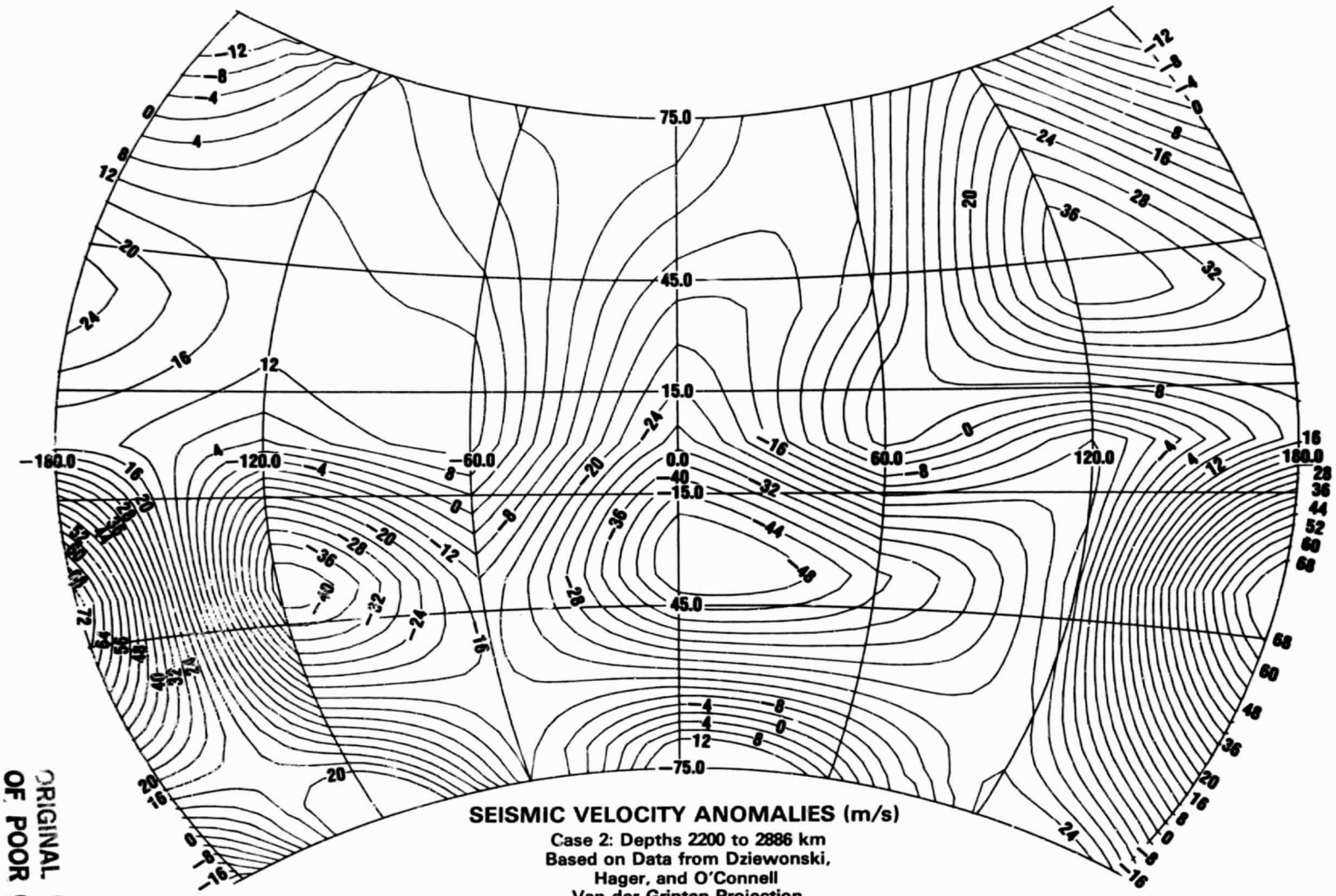
Case 2: Depths 1500 to 2200 km
Based on Data from Dziewonski,
Hager, and O'Connell
Van der Grinten Projection

B. E. Lowrey
F. T. Heuring

Goddard Space Flight Center

1978

ORIGINAL PAGE IS
OF POOR QUALITY



SEISMIC VELOCITY ANOMALIES (m/s)

Case 2: Depths 2200 to 2886 km
Based on Data from Dziewonski,
Hager, and O'Connell
Van der Grinten Projection

B. E. Lowrey
F. T. Heuring

Goddard Space Flight Center

1978

ORIGINAL PAGE IS
OF POOR QUALITY

BIBLIOGRAPHIC DATA SHEET

1. Report No.	2. Government Accession No.	3. Recipient's Catalog No.
TM 79722		

4. Title and Subtitle	5. Report Date
A Geophysical Atlas For Interpretation of Satellite-Derived Data	February 1979
	6. Performing Organization Code
7. Author(s)	8. Performing Organization Report No.
Paul D. Lowman, Jr. and Herbert V. Frey	
9. Performing Organization Name and Address	10. Work Unit No.
Geophysics Branch Goddard Space Flight Center Greenbelt, MD 20771	11. Contract or Grant No.
	13. Type of Report and Period Covered
12. Sponsoring Agency Name and Address	
same as above	14. Sponsoring Agency Code

15. Supplementary Notes

16. Abstract

This Atlas is a compilation of maps of global geophysical and geological data, plotted on a common scale and projection. The maps include satellite gravity, magnetic, seismic, volcanic, tectonic activity, and mantle velocity anomaly data. The Bibliographic references for all maps are included.

17. Key Words (Selected by Author(s))	18. Distribution Statement
Geophysics, Tectonic, Volcanism, Seismology, Mantle Structure, Geopotential Data	

19. Security Classif. (of this report)	20. Security Classif. (of this page)	21. No. of Pages	22. Price*

*For sale by the National Technical Information Service, Springfield, Virginia 22151.

GSFC 25-44 (10/77)